Enterococcus faecalis-derived lactic acid facilitates persistent and polymicrobial wound infections by suppressing macrophage activation

Ronni A. G. da Silva[1,2], Brenda Yin Qi Tien[2], Patrick Hsien Neng Kao[2], Cenk Celik[3], Ai Zhu Casandra Tan[2], Muhammad Hafiz Ismail[2], Guangan Hu[4], Kelvin Kian Long Chong[2], Guillaume Thibault[3,4], Jianzhu Chen[1,5], Kimberly A. Kline[1,2,6*]

[1] Singapore-MIT Alliance for Research and Technology, Infectious Disease Interdisciplinary Research Group, Singapore

[2] Singapore Centre for Environmental Life Sciences Engineering, Interdisciplinary Graduate School, Nanyang Technological University, 60 Nanyang Drive, Singapore 637551.

[3] School of Biological Sciences, Nanyang Technological University, Singapore

[4] Mechanobiology Institute, National University of Singapore, Singapore

[5] Koch Institute for Integrative Cancer Research and Department of Biology, Massachusetts Institute of Technology, Cambridge, MA, United States of America

[6] Department of Microbiology and Molecular Medicine, Faculty of Medicine, University of Geneva, Switzerland

[*]Correspondence: Kimberly.Kline@unige.ch

Summary

Macrophage activation is critical for the innate immune response, and its suppression by pathogens represents a significant barrier to immune clearance. Here we identify *E. faecalis*-derived lactic acid as a key factor in suppressing macrophage activation via extracellular acidification. We demonstrate that *E. faecalis* mutants lacking lactate dehydrogenase (*ldh*), essential for lactic acid production and extracellular pH reduction, fail to suppress NF-κB. Mechanistically, *E. faecalis*-derived lactic acid acts via MCT-1 and GPR81, to impair ERK and STAT3 phosphorylation, leading to reduced STAT3 binding to the *Myd88* promoter and reduced MyD88 protein levels, and ultimately to reduced NF-κB activity in macrophages. Consequently, in a wound infection model, the immunosuppressive microenvironment created by *E. faecalis* promotes long-term virulence and the virulence of co-infecting bacteria such as *Escherichia coli.* These findings highlight that bacterial-derived lactic acid contributes to the subversion of host immunity to promote persistent and polymicrobial infections.

Introduction

Enterococcus faecalis are commensal, lactic acid producing, Gram-positive bacteria that are ubiquitous in the healthy human gastrointestinal tract [1]. However, it is also an opportunistic pathogen in the nosocomial environment, particularly among immunocompromised individuals, with mortality rates exceeding 50% in these susceptible populations due to infection [2, 3]. *E. faecalis* infections are often polymicrobial in nature with two or more species present at the infection site, especially in catheter associated urinary tract infections (CAUTI) and wound infections [4-6]. Treatment of *E. faecalis* infections has become increasingly difficult due to their

acquired antibiotic resistance, antibiotic tolerance associated with their ability to form biofilm in the host, and intracellular survival [4, 7-9].

The nuclear factor kappa-light-chain-enhancer of activated B cells (NF-κB) pathway is a key regulator of the immune response to bacterial or viral infections [10-12]. Stimuli, such as lipopolysaccharide (LPS) or lipoteichoic acid (LTA), are recognized by co-receptors, including CD14 and pattern recognition Toll-like receptors (TLRs), inducing TLR dimerization and cargo internalization. This process, mediated by downstream adaptor proteins such as MyD88, activates the IκB kinase (IKK) complex [13]. The IKK complex phosphorylates IκB, leading to its ubiquitin-dependent degradation and release of NF-κB (typically a p65/p50 dimer), which then translocates to the nucleus and subsequently drives the expression of genes involved in immunity, inflammation, and cell survival [10].

To colonize and persist within the human host, *E. faecalis* deploys multiple strategies to evade immune clearance, including biofilm formation to hinder phagocytosis by immune cells, and prolonged survival within macrophages and neutrophils [8, 9, 14-19]. Additionally, *E. faecalis* strains isolated from the gastrointestinal tract of healthy human infants can suppress mitogen-activated protein kinase (MAPK) and NF-κB signaling, as well as interleukin 8 (IL-8) expression in intestinal epithelial cells *in vitro* [20, 21]. We previously demonstrated that *E. faecalis* infection of macrophages cells (RAW 264.7) *in vitro* at lower multiplicities of infection (MOI 1), but not higher (MOI 100) activate NF-κB signaling [22]. In addition, *E. faecalis* suppresses lipopolysaccharide (LPS) or lipoteichoic acid (LTA)-mediated NF-κB activation in the same cell line in a dose-dependent manner [22]. However, the bacterial and host

75 factors involved in the suppression of the NF-κB activation in macrophages by *E.*
76 *faecalis* infection were not identified.
77
78 In this study, we identified *E. faecalis* lactate dehydrogenase and its lactic acid product
79 as critical factors in macrophage suppression. Acting through the pH-sensitive lactate
80 transporter MCT-1 and the lactate sensor GPR81, *E. faecalis*-derived lactic acid
81 lowers the extracellular pH, reducing expression of MyD88 via impaired STAT3 activity
82 and preventing phosphorylation of key immune signaling proteins, ultimately blocking
83 NF-κB activation. During mammalian infection, lactic acid-mediated immune
84 suppression promotes persistent *E. faecalis* wound infection. Moreover, *E. faecalis*-
85 mediated immune suppression promotes *E. coli* growth during mixed species wound
86 infection. These findings advance our understanding of *E. faecalis* pathogenesis and
87 identify potential targets for immunotherapeutic strategies aimed at improving
88 treatment and prevention of recalcitrant infections.
89
90

91 ## Results

92

93 ### *E. faecalis* infection suppresses the antibacterial response of macrophages

94
95 We previously demonstrated that *E. faecalis* can suppress LPS- and LTA-mediated
96 NF-κB activation in RAW 264.7 macrophages in a dose-dependent manner without
97 causing host cell cytotoxicity [22]. To further investigate this immunosuppression, we
98 infected RAW 264.7 macrophages with *E. faecalis* strain OG1RF (hereafter called *E.*
99 *faecalis*) (MOI 1, 10 and 100) in the presence or absence of LPS followed by RNA
100 sequencing. Gene set enrichment analysis (GSEA) revealed that while *E. faecalis*

101 infection at MOI 100 enriched for pathways linked to the immune response to bacteria,
102 *E. faecalis* suppressed pathways associated with positive immune regulation and
103 defense responses in LPS-treated cells, **(Fig. 1A, SI 1-3)**. To explore how *E. faecalis*
104 interferes with NF-κB signaling, we examined transcripts of key genes in this pathway.
105 LPS alone increased transcripts that encode the LPS co-receptor CD14 [23], the NF-
106 κB transcription factor p65, and the transcription factor p50 precursors p100 and p105
107 **(Fig. 1B, Table S1, SI 4-6)**. *E. faecalis* significantly suppressed some of these LPS-
108 induced transcripts, with *Myd88* expression reduced ~2-fold lower in MOI 100-infected
109 LPS-untreated macrophages and nearly 4-fold lower in MOI 100-infected LPS-treated
110 macrophages compared to controls **(Fig. 1B, Table S1)**. This suppression may explain
111 why NF-κB is inactive following MOI 100 infection, despite higher transcript levels of
112 genes encoding p65, p100 and p105 compared to uninfected cells **(Fig. 1B, Table S1,**
113 **SI 4-6)**. Consistent with transcriptional findings, MyD88 protein levels were also lower
114 in MOI 100-infected macrophages with or without LPS. Predictably, downstream
115 phosphorylated proteins TAK1, IKK, IκBα, and p65 were also reduced, whereas the
116 levels of the unphosphorylated proteins of TAK1, IKKα and p65 were unchanged **(Fig.**
117 **1C and Fig. S1A)**.
118
119 Since MyD88 also activates AP-1 **(Fig. S1B)**, we investigated components of this
120 pathway, including ERK, c-Jun N-terminal kinases (JNK), p38, and AP-1 (c-Jun and
121 c-Fos). While LPS did not affect AP-1 pathway transcript levels **(Fig. 1B, Table S1)**,
122 MOI 100 infection reduced p38 transcripts compared to uninfected macrophages. In
123 LPS-treated cells, MOI 100 infection decreased *Fos* (encoding c-Fos) transcripts
124 relative to controls. Protein analysis showed significantly reduced phosphorylated
125 ERK at MOI 100, regardless of LPS presence **(Fig. 1C)**, while total and

126 phosphorylated levels of p38 and JNK, as well as total ERK levels were unaffected
127 **(Fig. 1C and S1C)**. Minimal changes in phosphorylated c-Jun and c-Fos at MOI 100
128 suggest that *E. faecalis* likely interferes with AP-1 activation to a lesser degree than
129 with NF-κB **(Fig. S1C),** cumulatively suppressing macrophage activation.
130
131 To determine if *E. faecalis* affects other aspects of MyD88-related signaling, beyond
132 suppressing *Myd88* expression, we scrutinized the RNA-seq data to include a wider
133 range of immune signaling genes like pathogen recognition receptors. While *Tlr4*
134 transcript levels remained unchanged by *E. faecalis* infection, expression of *Cd14* was
135 reduced following 6 h of infection of LPS-treated cells, indicating that *E. faecalis* might
136 also impact cargo internalization, since CD14 mediates the LPS-induced
137 internalization of extracellular molecules [23] **(Fig. 1D and Table S1)**. We therefore
138 examined receptor endocytosis, but observed no marked difference in CD14
139 internalization, suggesting that *E. faecalis* infection-mediated suppression of NF-κB
140 cannot be explained by changes in CD14 levels and internalization **(Fig. 1D)**. Similarly,
141 *E. faecalis* infection had no effect on TLR2 internalization with or without LTA **(Fig.**
142 **S1D)**. Taken together, these data show that *E. faecalis* infection suppresses NF-κB
143 activation in macrophages by reducing MyD88 protein levels preventing the
144 downstream phosphorylation cascade and therefore leading to NF-κB suppression.
145
146
147 ***E. faecalis*-derived lactic acid is essential for NF-κB suppression in**
148 **macrophages**
149 To investigate the bacterial factors involved in suppression of macrophage activation,
150 we screened a ~15,000 member *E. faecalis* mariner transposon library [24] for mutants

151 that failed to suppress LPS-induced NF-κB activation in RAW 264.7 macrophages.
152 We identified 151 transposon mutants in our primary screen **(Fig. S2A)** which were
153 then subjected to secondary analyses for growth defects **(Fig. S2B)**, leading to a final
154 list of 47 transposon mutants that failed to suppress NF-κB activation **(Fig. 2A, Table**
155 **S2)**. Since bacterial growth was conducted in media containing a pH indicator, we
156 noted that 18 of 47 mutants failed to acidify the media as a function of growth as
157 compared to WT *E. faecalis* **(Fig. 2A).** Among these, we identified *ldh1*
158 (OG1RF_10199), encoding lactate dehydrogenase (LDH) **(Fig. 2A)**, which reduces
159 pyruvate to L-lactate to generate NAD^+ for ongoing glycolysis in *E. faecalis* [25, 26]. L-
160 lactate is released from *E. faecalis* in the form of lactic acid (LA), which is subsequently
161 deprotonated to L-lactate, releasing a hydrogen ion (H^+) and in turn lowering the pH in
162 the surrounding environment. Since acidification is a defining feature of *E. faecalis*
163 metabolism due to the release of lactic acid [27], we decided to further investigate the
164 impact of LDH on NF-κB activation.
165
166 The *E. faecalis* genome contains two LDH genes, *ldh1* and *ldh2,* where LDH1 plays
167 the major role in lactic acid production under laboratory conditions as compared to
168 LDH2 [25]. As predicted, and confirming the result of the transposon screen, infection
169 of RAW 264.7 macrophages with Δ*ldh1* or the Δ*ldh1*Δ*ldh2* double mutant (hereafter
170 called Ldh), failed to suppress LPS-induced NF-κB activation as compared to WT *E.*
171 *faecalis*, Δ*ldh2,* or *ldh1* complementation strains **(Fig. 2B).** Failure to suppress
172 macrophage activation was not due to a growth defect of the *ldh1* mutant, whether
173 grown in BHI or cell culture medium **(Fig. S3A-B)**. Lactic acid accumulated in culture
174 supernatants of WT *E. faecalis* infection in an MOI-dependent manner after 6 h of
175 incubation with RAW264.7 cells **(Fig. S3C-D)**. In contrast to WT *E. faecalis*, infection

176 with either the Δ*ldh1* and Ldh mutants produced less lactic acid and, consequently,
177 acidified the environment at a slower rate than WT *E. faecalis* **(Fig. S3E-G)**. Consistent
178 with previous reports, Δ*ldh2* was attenuated for lactate release **(Fig. S3E-G)** [25, 28].
179
180 To confirm that LDH-mediated macrophage suppression was not specific to RAW
181 264.7 macrophages, we assessed the release of the NF-κB-regulated cytokine IL-6
182 from murine bone marrow-derived macrophages (BMDM) infected with Δ*ldh1* and Ldh
183 mutants compared to WT *E. faecalis* **(Fig. 2C)**. Similar to RAW 264.7 macrophages,
184 infection with both the WT or the Δ*ldh1* complemented strains had no effect on the
185 release of IL-6 by BMDMs, whereas infection of LPS-treated cells with either Δ*ldh1* or
186 Ldh stimulated IL-6 production **(Fig. 2C)**. Additionally, infection of BMDMs and the
187 human monocyte-like cell line THP-1 with WT *E. faecalis* also decreased the levels of
188 MyD88 and p-ERK while the levels remained similar to uninfected cells following
189 infection with the Ldh mutant **(Fig. S3H)**. Accordingly, we also detected higher levels
190 of p-ERK and p-p65 in macrophages infected with the Ldh mutant as compared to WT
191 *E. faecalis*, further supporting a role for LDH in *E. faecalis* suppression of macrophage
192 NF-κB activation, which in turn leads to lower levels of pro-inflammatory cytokines **(Fig.**
193 **S3I)**. Multiplex cytokine analysis of RAW264.7 cells also confirmed reduced levels of
194 pro-inflammatory cytokines (IL-6, IL-12 p70 and IFNγ) and chemokines (CCL3, CCL4,
195 CCL5, CSF2 and CSF3) for WT-infected macrophages in presence of LPS **(Fig. S3J)**.
196 Furthermore, supplementation of macrophages infected with the Ldh mutant with a
197 minimum of 20 mM lactic acid restored suppression of LPS-induced NF-κB activation
198 to similar levels as WT *E. faecalis* **(Fig. 2D)**. Under non-infectious conditions, lactic
199 acid concentrations above 40 mM were sufficient to suppress LPS-induced NF-κB
200 activation **(Fig. 2E)** without compromising macrophage viability **(S3D)**. Moreover, WT

201 *E. faecalis* suppressed LPS-induced NF-κB activation even in cells pre-activated with
202 LPS for 1 h prior to infection **(Fig. S4A-B)**. As expected, the Ldh mutant failed to
203 suppress NF-κB activation independent of LPS pre-exposure **(Fig. S4A-B)**. Overall,
204 these results demonstrate that *E. faecalis* suppression of NF-κB activation in
205 macrophages is mediated by LDH-derived LA.
206
207 ***E. faecalis* reduction of extracellular pH is critical for suppressing the**
208 **macrophage response to infection**
209 Among the 47 transposon mutants that failed to suppress macrophage activation, 18
210 did not acidify the medium as well as WT *E. faecalis*. However, of these 18 "weakly
211 acidifying" mutants, only 11 produced less lactate **(Fig. 2A)**, indicating that overall
212 acidification - rather than lactic acid production alone - contributes to suppressing LPS-
213 induced NF-κB activation during *E. faecalis* infection. Given that lactic acid production
214 both lowers extracellular pH and increases extracellular lactate levels, we examined
215 whether lactate or low pH by lactic acid mediates the suppression of NF-κB activation.
216 Supplementation with 40 mM lactic acid effectively suppressed NF-κB activation,
217 whereas 40 mM sodium L-lactate did not, indicating that low pH, rather than lactate,
218 drives the suppression phenotype **(Fig. 3A)**. To confirm this, we mimicked the acidity
219 of filtered bacterial-free Ldh supernatants to pH 6.4 (the pH observed at MOI 100)
220 using HCl or neutralized WT supernatants to pH 7.8 (the pH observed at MOI 1) with
221 Tris. These supernatants were collected from *E. faecalis* cultures inoculated at various
222 MOI in cell culture medium and incubated for 6 h mirroring infection assays. All
223 acidified bacteria-free supernatants suppressed LPS-induced NF-κB activation across
224 all MOIs, while neutralized supernatants failed to do so **(Fig. 3B-C)** in the absence of
225 cytotoxicity **(S5B-C)**. Consistent with previous reports [29], acidifying cell culture

226 media to pH 6.4 using HCl or phosphoric acid (H_3PO_4) suppressed LPS-induced NF-
227 κB activation without affecting macrophage viability **(Fig. 3D and S5D).** Adjusting Ldh
228 mutant cell-free supernatants with HCl or H_3PO_4 to pH 6.4 also rescued suppression
229 of LPS-induced NF-κB activation to levels comparable to WT *E. faecalis* **(Fig. S5E-F)**.
230 p-p65 levels were also reduced in macrophages infected with the Ldh mutant with LPS
231 co-stimulation when supplemented either with lactic acid or HCl, compared to those
232 without acid supplementation **(Fig. S5G)**.
233
234 Since *E. faecalis* can persist and replicate within macrophages [9, 30], we investigated
235 whether intracellular *E. faecalis* contributed to NF-κB suppression. We therefore
236 infected macrophages with *E. faecalis* at different MOI for 3 h and killed the
237 extracellular *E. faecalis* with gentamicin and penicillin G as previously described [9].
238 In the absence of extracellular *E. faecalis* and its associated acidification of the
239 medium, we observed that NF-κB activation was significantly increased at all MOIs
240 during intracellular infection, without significant cell death **(Fig. S6A-B).** In fact, *E.*
241 *faecalis* infection resulted in higher NF-κB activation than the LPS positive control **(Fig.**
242 **S6A)**. Together, our results suggest that extracellular acidification, rather than lactate
243 levels or intracellular infection, is important for the immune modulation mediated by *E.*
244 *faecalis* in macrophages.
245
246 ***E. faecalis*-lowered pH suppresses MyD88 expression by disrupting STAT3**
247 **activity**
248 To understand the mechanism by which *E. faecalis*-mediated acidification impacts NF-
249 κB activation, we focused on the reduction of MyD88 levels, which would give rise to
250 the observed downstream signaling defects. STAT3 is a transcription factor that

251 regulates *Myd88* transcript levels [31]. STAT3 activation depends on its
252 phosphorylation [32] by ERK at serine 727, preceded by ERK phosphorylation by MEK
253 [33-35]. STAT3 activity can also be inhibited by acetylation [31]. Western blot analysis
254 following 6 h of *E. faecalis* infection showed reduced MyD88 levels in WT infections
255 compared to uninfected or Ldh-infected macrophages, along with reduced ERK, MEK,
256 and STAT3 phosphorylation in WT-infected macrophages **(Fig. 4A)**. Total STAT3
257 protein levels were slightly reduced in WT-infected macrophages whereas total MEK
258 protein levels were unchanged.
259
260 To evaluate whether *E. faecalis* infection reduces STAT3 binding to the *Myd88*
261 promoter, we performed chromatin immunoprecipitation (ChIP) followed by qPCR.
262 Using the Eukaryotic Promoter Database (EPD), we identified six potential STAT3
263 binding sites near the *Myd88* transcription starting site that could be grouped and
264 probed based on their proximity: region 1 (R1; -1147 and -1065), region 2 (R2; -61
265 and -23) and region 3 (R3; 386 and 488). STAT3 binding was reduced at these regions
266 in WT *E. faecalis* infected macrophages treated with LPS, whereas Ldh-infected LPS-
267 treated macrophages showed no reduction **(Fig. 4B)**. These findings indicate that *E.*
268 *faecalis* suppresses *Myd88* expression by interfering with STAT3 activity. Further,
269 lactic acid alone was sufficient to reduce STAT3 binding at these sites, consistent with
270 a model in which *E. faecalis*-derived acidification governs *Myd88* expression by
271 impairing STAT3 activity.
272
273 Since STAT1 may also regulate *Myd88* transcript levels [36], we conducted NF-κB
274 reporter assays with MEK, STAT1 and STAT3 inhibitors and agonists to assess their
275 roles in NF-κB signaling **(Fig. 4C-D and S7A-C),** at concentrations that do not cause

276 cytotoxicity **(Table S3)**. RAW264.7 cells were pre-treated with each compound for 30
277 min to prime the cells. STAT3 inhibition with Stattic impaired NF-κB activation in the
278 presence of LPS, regardless of *E. faecalis* infection **(Fig. 4C)**. In addition, consistent
279 with MEK's role in the phosphorylation of STAT3 and, ultimately, in regulating NF-κB
280 [37], pharmacological inhibition of MEK with Selumetinib (Selu) suppressed LPS-
281 induced NF-κB **(Fig. S7A)**. By contrast, STAT1 inhibition with Fludarabine (Fluda)
282 reduced, but did not completely abolish, NF-κB activation **(Fig. S7B)**, indicating that
283 STAT3 plays a more critical role in NF-κB activation than STAT1. Moreover, LPS-
284 induced NF-κB activation was restored in *E. faecalis*-infected cells treated with the
285 STAT3 agonist ML115 but not with the STAT1 agonist 2NP **(Fig. 4D and Fig. S7C)**,
286 reinforcing the central role of STAT3 in NF-κB activation. Functionally, treatment of
287 macrophages with ML115 to overcome *E. faecalis*-mediated STAT3 suppression
288 enhanced intracellular bacterial clearance by ~1-log CFU, whereas treatment with 2NP
289 did not **(Fig. 4E)**. In a murine wound infection model, topical application of the infected
290 wounds with the STAT3 agonist ML115 reduced *E. faecalis* CFU by 1.1-log compared
291 to PBS treatment **(Fig. 4F)**. Collectively, these results demonstrate that *E. faecalis*
292 interferes with STAT3 activity to suppress *Myd88* transcription, thereby inhibiting NF-
293 κB activation and effective immune clearance.
294

295 **MCT1 and GPR81 mediate NF-κB suppression in *E. faecalis*-infected**
296 **macrophages**

297 Macrophages express several receptors that can sense lactate gradients and
298 extracellular pH variation [38, 39]. To investigate the role of pH-sensitive lactate
299 transporters and sensors during *E. faecalis* infection, we used RNA silencing in the
300 RAW 264.7 reporter cell line to knock down the genes that encode for

301 monocarboxylate transporter 1 (MCT1), G protein-coupled receptor 81 (GPR81, also
302 known as hydroxycarboxylic acid receptor 1), and G protein-coupled receptor 65
303 (GPR65). Individual knockdowns of these genes partially restored NF-κB activation in
304 *E. faecalis*-infected macrophages, with or without LPS **(Fig. S8A-C)**. Notably, double
305 knockdown of *Mct-1* and *Gpr81*, as well as a triple knockdown of *Mct-1*, *Gpr81* and
306 *Gpr65*, restored NF-κB activation in macrophages treated with LPS in the presence *E.*
307 *faecalis* **(Fig. 5A-B)**. By contrast, double knockdown of *Gpr65* with either *Mct-1* or
308 *Gpr81* did not yield similar effects **(Fig. S8D-E)**, suggesting that GPR65 plays a lesser
309 role in sensing lactate/protons and mediating NF-κB suppression during *E. faecalis*
310 infection. As a control, GAPDH knockdown had no effect on NF-kB activation in LPS-
311 treated macrophages or suppression of NF-kB activation in *E. faecalis*-infected
312 macrophages **(Fig. S8F)**. The gene knockdown efficiencies were confirmed by RT-
313 PCR **(Fig. S9)**.
314 To further verify the roles of the MCT and GPCR proteins in NF-κB suppression, we
315 treated macrophages with the MCT-1/MCT-4 inhibitor 2-cyano-3-(4-hydroxyphenyl)-2-
316 propenoic acid (CHC) and the adenylyl cyclase inhibitor MDL-12330A hydrochloride
317 (MDL-12) in the presence and absence of both *E. faecalis* and LPS **(Fig. S10A-C)**.
318 MDL-12 treatment alone slightly reduced NF-κB activation **(Fig. S10B),** consistent with
319 the role of cyclic adenosine monophosphate (cAMP) in NF-κB signaling [40]. However,
320 combined treatment of CHC and MDL-12 restored NF-κB activation in *E. faecalis*-
321 infected macrophages to levels comparable to LPS treatment alone **(Fig. S10C)**
322 indicating that G protein-coupled receptors and MCT-1 mediate lactic acid signal to
323 suppress macrophages activation.
324

325 Lactate from *Staphylococcus aureus* (*S. aureus*) biofilms alters histone acetylation in
326 leukocytes by increasing histone deacetylase 6 (HDAC6) activity and reducing
327 HDAC11 activity [41]. To assess HDAC contribution to lactic acid-mediated NF-κB
328 suppression in macrophages during *E. faecalis* infection, we measured histone
329 acetylation (H3Ac) in uninfected macrophages and macrophages infected with either
330 *E. faecalis* WT or the Ldh mutant. H3Ac levels were unchanged in WT-infected
331 macrophages but decreased in Ldh-infected cells **(Fig. S11A).** Treatment with the
332 HDAC pan inhibitor trichostatin A (trichoA) partially restored NF-κB activation in LPS-
333 treated, *E. faecalis*-infected macrophages **(Fig S11B)**. Selective inhibition of HDAC6
334 via tubastatin A (tubA) increased NF-κB activation in WT *E. faecalis*-infected LPS-
335 treated macrophages, but not in *E. faecalis*-infected cells **(Fig S11C**), suggesting that
336 HDAC6 minimally impacts NF-κB suppression. Inhibition of other HDACs (HDAC11,
337 HDAC8, HDAC4/5/7/9, and HDAC1) failed to prevent NF-κB suppression **(Fig S11D-**
338 **G)**. Together these results show that MCT-1 and GPR81 play major roles in NF-κB
339 suppression during *E. faecalis* infection, while HDACs have a minimal role.
340
341 ***E. faecalis* lactate dehydrogenase contributes to *E. faecalis* persistence in**
342 **wound infections**
343 *E. faecalis* infection suppresses the immune response and impairs healing in a murine
344 model of wound infection [42]. Hence, we reasoned that LDH-mediated immune
345 modulation is important for *E. faecalis* survival in wounds. To test this, wounds were
346 inoculated with either WT *E. faecalis* or the Ldh mutant. Both strains showed similar
347 survival at 24 hpi **(Fig. 6A)**, despite LDH-dependent depletion of lactate in wound
348 tissues at the same time point **(Fig. S12A)**. At 7 dpi, CFU of the Ldh mutant were ~1-
349 log lower than those of WT **(Fig. 6B)**, indicating a stronger role for LDH in persistent

350 rather than in acute infection. Analysis of p-p65, p-ERK, and MyD88 in both uninfected
351 and infected wounds revealed a reduction in p-ERK at 24 hpi and all three proteins at
352 7 dpi for WT, but not Ldh mutant, infected wounds **(Fig. 6C)**. These results show that
353 LDH contributes significantly to persistent *E. faecalis* wound infections by modulating
354 immune signaling pathways.

355 ***E. faecalis* LDH-mediated immune suppression promotes *E. coli* survival during**
356 **mixed species infection**

357 We previously showed that co-infection with *E. faecalis* enhances *E. coli* virulence and
358 growth in a mouse wound infection model [43]. We hypothesized that this phenotype
359 is partly due to *E. faecalis*-mediated immune suppression, creating a favorable
360 environment for *E. coli*. To test this, we examined whether infection with the Ldh
361 mutant fails to suppress NF-κB in the presence of *E. coli*. In fact, infection of RAW
362 264.7 macrophages with the Ldh mutant resulted in higher NF-κB activation compared
363 to co-infection with WT *E. faecalis*, indicating that the Ldh mutant is less effective at
364 suppressing *E. coli*-induced NF-κB activation **(Fig. 7A)**. During mixed-species wound
365 infection, co-inoculation with a 1:1 ratio of *E. coli* and either WT *E. faecalis* or the Ldh
366 mutant showed similar *E. faecalis* CFU regardless of *E. coli* presence at 24 hpi **(Fig.**
367 **7B)**. However, *E. coli* growth was significantly enhanced during co-infection with WT
368 *E. faecalis* but not with the Ldh mutant **(Fig. 7C)**. To exclude lactate as a nutrient
369 source for *E. coli*, we tested its growth *in vitro* with increasing lactate concentrations
370 and found no growth enhancement **(Fig. S12B)**. These findings indicate that LDH-
371 mediated immune suppression by *E. faecalis* promotes *E. coli* growth during wound
372 infection.

373

374

375 ## Discussion

376 *E. faecalis* is among the top five pathogens associated with hospital acquired
377 infections including CAUTI, central line-associated bloodstream infection and surgical
378 site infection [4, 44]. While previous studies focused on host inflammatory responses
379 at lower MOI [20, 45], we and others have shown that *E. faecalis* exhibits
380 immunomodulatory properties at higher MOI via mechanisms and bacterial factors that
381 were previously unclear [21, 22, 46]. Here we demonstrate that *E. faecalis* infection at
382 MOI 100 suppresses macrophage activation by interfering with STAT3 activity,
383 resulting in reduced MyD88 levels, and inhibition of downstream signaling events
384 required for NF-κB activation **(Fig. 8)**. Additionally, we identify *E. faecalis* lactate
385 dehydrogenase (LDH) and its lactic acid product as critical factors for macrophage
386 suppression and persistence in wounds, as well as for promoting *E. coli* growth during
387 co-infection.

388

389 Lactic acid production is a metabolic hallmark of *E. faecalis* fermentation [47]. *E.*
390 *faecalis* LDH catalyzes the reduction of pyruvate to L-lactate, which is exported as
391 lactic acid and deprotonates into L-lactate at physiological pH, reducing the local pH.
392 Here we show that *ldh1* is necessary, and its byproduct (lactic acid) is sufficient, to
393 suppress LPS-induced NF-κB activation. This may be why LDH-deficient *E. faecalis*
394 exhibit reduced virulence in systemic murine infections [26]. Similarly, LDH is
395 important for virulence of *S. aureus* in a murine sepsis model [48]. Lactic acid-induced
396 immunosuppression appears widespread; other lactic acid bacteria, such as
397 *Lactobacillus*, suppress NF-κB activation in macrophages and myometrial cells [49,
398 50]. While we focused on the role of LDH in this study, we identified additional mutants
399 that failed to suppress LPS-induced NF-κB activation despite acidifying the

400 environment, suggesting additional immune suppressive mechanisms, calling for
401 further investigation. Beyond infection, lactic acid contributes to immune suppression
402 in tumor microenvironments, inducing tissue acidosis that suppresses NF-κB activity,
403 through mechanisms involving pH changes and histone acetylation [51-62]. Here we
404 show that *E. faecalis* lactic acid-mediated suppression of MyD88 levels and
405 downstream signaling events can be mimicked by acidic conditions, driven by pH
406 effects rather than phosphorylation changes. These mechanisms may be context
407 dependent and warrant further study.
408
409 The MEK-ERK-STAT3 axis is disrupted by *E. faecalis*-derived lactic acid, reducing
410 STAT3 phosphorylation and binding to the *Myd88* promoter, consistent with previous
411 reports [31]. While other bacterial infections activate the MEK/ERK cascade for
412 oxidative and nitrosative bursts, endosomal trafficking, and proinflammatory
413 macrophage polarization [63-65], *E. faecalis* subverts this defense [66, 67].
414 *Salmonella typhimurium* and *Helicobacter pylori*, for example, induce STAT3
415 phosphorylation via secreted factors to alter immune responses [66]. We propose that
416 pH sensitive kinases, including MEK and ERK, are disrupted at lower intracellular pH,
417 inhibiting STAT3 activity [68]. Indeed, pH 6.2-6.4 reduces MEK and ERK
418 phosphorylation in fibroblasts [69]. Moreover, reduced IL-6 secretion from *E. faecalis*-
419 infected macrophages likely contributes to diminished STAT3 phosphorylation [70],
420 necessitating further exploration.
421
422 How then does extracellular *E. faecalis*-derived lactic acid exert these pH-driven
423 intracellular effects? We identified the host lactate transporter MCT-1 and the lactate
424 sensor GPR81 as mediators of NF-κB suppression during *E. faecalis* infection. MCT-

425 1 import of lactate mediates the inhibition of HDAC11 activity that leads to the
426 activation of HDAC6 to promote IL-10 release, whereas GPR81 sensing of
427 extracellular lactate prevents the activation of the transcription factor YAP and,
428 ultimately, elicits NF-κB suppression [71, 72]. Expression of the genes encoding MCT-
429 1 and GPR81 is pH-dependent [25-27]. Moreover, MCT-1 can transport both lactate
430 and protons, and both MCT-1 and GPR81 are activated at lower pH [38, 73]. Lactate
431 supplementation alone did not replicate *E. faecalis* LDH-mediated immune
432 suppression, suggesting that MCT-1/GPR81 activation is pH dependent. In turn, we
433 therefore propose that MCT-1 transport of protons into the cell disrupts MEK-ERK-
434 STAT3 phosphorylation. Initially, our hypothesis seems to contrast with a study
435 showing that lactic acid can induce phosphorylation of ERK in rat hepatocyte RLN-10
436 cells via GPR81 sensing [74]. Nonetheless, that study was conducted under adjusted
437 neutral pH, ultimately excluding the potential effect of pH on ERK phosphorylation.
438 Similarly, studies showing increased MEK and ERK phosphorylation via GPR81 used
439 sodium lactate, which does not lower pH in their experiments [75, 76]. Conversely,
440 others have observed that acidosis (pH 4-5) can activate ERK2, but not ERK1, in
441 human epidermoid squamous carcinoma A431 cells [77], whereas pH 6.6 can
442 increase the phosphorylation of ERK after 2 h of incubation but gradually inhibit
443 phosphorylation after 4 h in human prostate carcinoma epithelial 22Rv1 cells [78].
444 Similarly, pH 6.3 was observed to inhibit ERK phosphorylation in Jurkat cells after 24
445 h [79]. Altogether, these studies are consistent with our model that pH affects the
446 phosphorylation status of these kinases.
447
448 *E. faecalis* wound infections are immune suppressive and delay wound healing [42].
449 We show that *E. faecalis* LDH activity drives immune suppression, *E. faecalis*

450 persistence in wounds, as well as the growth of *E. coli* during co-infection. Given the
451 prevalence of infections caused by lactic acid producing bacteria [80, 81], as well as
452 their contribution to healthy microbiomes, additional studies are needed to determine
453 mechanistically how pH and lactate promote polymicrobial interactions more broadly.
454 Importantly, compounds that override this suppression and activate macrophage NF-
455 κB signaling during *E. faecalis* infection are effective to enhance macrophage
456 intracellular killing of bacteria [82, 83]. Here, we observed that the STAT3 agonist
457 ML115 was also effective both *in vitro* and *in vivo* to reduce the bacterial burden of *E.*
458 *faecalis* infection, further highlighting the therapeutic potential of immunomodulation
459 for immunosuppressive bacterial infections. Overall, a comprehensive understanding
460 of the immunological pathways affected by *E. faecalis* infection could inform new
461 strategies to mitigate persistent infections.

462
463

464 Materials and Methods

465 Bacterial strains and growth conditions

466 Uropathogenic *E. coli* (UPEC) strain UTI89 [84, 85] was grown overnight in Luria-
467 Bertani (LB) (Difco, France) broth or agar at 37°C under static conditions. *E. faecalis*
468 strain OG1RF [86] or *ldh* mutants [87] were grown statically in brain heart infusion
469 (BHI) (Becton, Dickinson, USA) broth or agar at 37°C overnight. Overnight cultures of
470 bacteria were centrifuged at 6,000 *g* for 5 minutes and resuspended in PBS at OD_{600}
471 0.7 (2 x 10^8 CFU/mL) for *E. faecalis* and at OD_{600} 0.4 (2 x 10^8 CFU/mL) for *E. coli*.

472

473 Genetic manipulations

474 To create deletion mutants, we used a thermosensitive shuttle plasmid pCGP213
475 which was isolated using the Monarch Plasmid Miniprep Kit (New England BioLabs
476 Inc., USA) following the manufacturer's instruction [87]. OG1RF genomic DNA is
477 isolated using Wizard Genomic DNA Purification Kit (Promega, USA) and Phusion
478 DNA polymerase (Thermo Fisher Scientific, Singapore) was used to amplify
479 approximately 1 kb upstream and downstream of the gene of interested in accordance
480 to manufacturer's protocol. Primers used in the study are listed in **Table S4**.
481 Subsequently, the amplified products were sewn together using the primers
482 dLDH1_For, dLDH1_Rev, dLDH2_For and dLDH2_Rev. *ldh1* and *ldh2* constructs
483 were then subcloned individually into pGCP213 using In-Fusion HD Cloning Kit using
484 (Clontech, Takara, Japan) following manufacturer's instruction. Deletion constructs
485 were then transformed into *E. coli* and correct transformants were selected at 37°C
486 under erythromycin (Sigma-Aldrich, St Louis, MO) pressure 500 µg/mL (MP, France).
487 The amplified plasmids were the purified from *E. coli* using the Monarch Plasmid
488 Miniprep Kit. The plasmids were then transformed into OG1RF using electroporation,
489 and the correct transformants were selected at 30°C under erythromycin pressure 25
490 µg/mL. Chromosomal integrations were selected by passaging 37°C in the absence
491 of erythromycin. The loss of *ldh1* or *ldh2* is then verified by PCR using primer pairs
492 LDH1_F, LDH1_R, LDH2_F and LDH2_R. Δ*ldh1*Δ*ldh2* was created by subcloning the
493 pGCP213-*ldh1* deletion construct into Δ*ldh2*. All deletion constructs were
494 subsequently confirmed using whole genomic sequence to ensure that only the gene
495 of interested is deleted in the absence of any spontaneous mutation.
496
497 **Growth kinetics and pH curve**

498 Bacterial cultures were grown as described above and overnight cultures were
499 normalized to obtain a final concentration of 10^3 cells/mL before inoculating at 1:25
500 ratio into 200 µL of either BHI or DMEM supplemented with 10% FBS. Subsequently,
501 growth rates were measured by recording OD 600 over 20 h at 37°C using a microplate
502 reader (Tecan infinite M200 Pro, Switzerland).
503
504 For pH measurements, bacterial cultures were grown and normalized to 3.4 x 10^7
505 cells/mL (assuming MOI 100 for 10^6 macrophages) in DMEM supplemented with 10%
506 FBS. The pH was then measured at 1-h interval for up to 6 h, and subsequently
507 measured at 8 h and 24 h using a digital pH meter (Sartorius, Germany).
508
509 **Cell culture**
510 RAW 264.7 cells derived from RAW 264.7 macrophages (Invivogen, USA), containing
511 a plasmid encoding a secreted embryonic alkaline phosphatase (SEAP) reporter
512 under transcriptional control of an NF-κB-inducible promoter, were cultivated in
513 Dulbecco Modified Eagle medium (DMEM) containing 4500 mg/L high glucose (1X)
514 with 4.0 nM L-glutamine, without sodium pyruvate (Gibco, Thermo Fisher Scientific,
515 Singapore) and supplemented with 10% fetal bovine serum (FBS; PAA) supplemented
516 with 200 µg/mL Zeocin (Gibco, Thermo Fisher Scientific, Singapore), at 37˚C in 5%
517 CO_2.
518
519 **Bone marrow-derived macrophages (BMDM) isolation and cultivation**
520 BMDMs were harvested according to previously published protocol [88]. Briefly,
521 femurs were harvested from 6 to 10 weeks old C57BL/6J mice (InVivos Pte. Ltd.,
522 Singapore). Following euthanasia, the legs were first sprayed with 70% ethanol before

523 dissection and removing the skin and muscles. The bone was then placed in 70%
524 ethanol and transferred into a sterile flow hood. Subsequently, the bone was cut using
525 scissor and bone marrow was flushed out with cell culture media (containing DMEM
526 with 10% FBS and supplemented with 100 U/mL penicillin and 100 µg/mL
527 streptomycin (Gibco, Thermo Fisher Scientific, Singapore) using a 26G needle into a
528 sterile falcon tube (Becton, Dickinson and Company, Franklin Lakes, NJ).
529 Subsequently, cell suspension was centrifuged at 500 G for 5 mins and the
530 supernatant was removed. The cell pellet was then resuspended in 1X RBC Lysis
531 Buffer (eBioscience, Thermo Fisher Scientific, Singapore) for lysis of erythrocytes.
532 After 5 mins, PBS was added to inactivate the lysis buffer before centrifuging the cell
533 suspension. Supernatant was discarded, and cell pellet was resuspended in cell
534 culture media supplemented with 100 ng/mL macrophage colony-stimulating factor
535 (M-CSF) (Biolegend, San Diego, USA), 100 U/mL penicillin and 100 µg/mL
536 streptomycin. Cells were adjusted to 2 x 10^6 cells/mL and seeded into T175 flask (Nunc,
537 Thermo Fisher Scientific, China) and incubated at 37°C with 5% CO_2. After 2-3 days,
538 cells were washed, and fresh cell culture media supplemented with 100 ng/mL M-CSF
539 was added. Macrophages are fully differentiated after 6 to 7 days, ready for
540 experimental use.
541
542 **RAW 264.7 macrophage or BMDM infection**
543 RAW 264.7 cells and BMDM were seeded into 96-well and 6-well microtiter plates
544 (Nunc, Thermo Fisher Scientific, Singapore) with cell density of 1 x 10^5 or 1 x 10^6
545 cells/well respectively in antibiotic free media (DMEM with 10% heat inactivated FBS)
546 and incubated overnight at 37°C with 5% CO_2 when necessary. Following overnight
547 incubation, the cells were washed once with PBS and fresh media was added. The

548 SEAP reporter assay was established by empirically defining the minimal agonist LPS
549 concentration that induced the maximum SEAP activity in the absence of cell death.
550 Cells were stimulated using LPS purified from *E. coli* O111:B4 (Sigma-Aldrich, St
551 Louis, MO) (100 ng/mL) as positive control, or media alone as a negative control. RAW
552 264.7 cells were infected with *E. faecalis* (at MOI of 100:1, 10:1 and 1:1) for 6 h with
553 or without TLR agonists. For co-infection experiments, RAW 264.7 cells were
554 simultaneously infected with *E. coli* UTI89 (MOI of 0.125:1) and *E. faecalis* (MOI of
555 100:1).
556
557 **ChIP-qPCR and histone H3 acetylation assay**
558 For each sample, chromatin immunoprecipitated DNA was captured using a STAT3
559 Rabbit mAb (D3Z2G; CST) and a high-sensitivity ChIP kit (Cat. #ab185913; Abcam)
560 according to the manufacturer's instructions and as inspired by [72] .The captured and
561 purified DNA was prepared for ChIP-qPCR, and specific primers (**Table S3**) were
562 designed for the sites that we identified as potential STAT3 binding sites near the
563 *Myd88* transcriptional starting site (TSS). The prediction of STAT3 binding sites
564 around the *Myd88* TSS was made using the Eukaryotic Promoter Database (EPD)
565 (https://epd.expasy.org/epd/). We identified six potential STAT3 binding sites near the
566 *Myd88* TSS (-1147, -1065, -61, -23, 386 and 488). We named them region 1 (R1, -
567 1147 and -1065), region 2 (-61 and -23), and region 3 (386 and 488). For R1, we
568 designed primers that covered from region -100 to 0; for R2 from -1030 to -1182 and
569 R3 from 362 to 464 **(Table S4)**. qPCR was performed for each primer set. Amplification
570 was performed with KAPA SYBR Fast (Kapa Biosystems) with specific primers **(Table**
571 **S4)** and detected by StepOnePlus Real-Time PCR machine (Applied Biosystems).
572 Relative quantification was performed using the delta-delta method [89] with calibrator

573 primers that interrogate the *Gapdh* gene. Positive control was established for an RNA
574 polymerase binding site for the *Gapdh* gene. To measure the levels of histone H3
575 acetylation of samples infected with *E. faecalis*, the histone H3 acetylation assay Kit
576 (#ab115102, Abcam) was used as per the manufacturer's instructions.
577
578 **Flow cytometry**
579 To assess CD14 and TLR2 surface levels, flow cytometry was performed as described
580 in [23, 83]. RAW 264.7 cells were either infected or treated with LPS (1 μg/mL) or LTA
581 (10 μg/mL) alone or in combination for 30 min to 120 min before CD14 (LPS) and
582 TLR2 (LTA) endocytoses were examined by flow cytometry. Cells (10^7 per sample)
583 were then incubated with 10 µL of Fc-blocker (anti-CD16/CD32 antibody; BioLegend)
584 for 30 min, followed by incubation with a CD14 and TLR2 marker-conjugated
585 antibodies (BioLegend) (1:100 dilution) for 30 min at room temperature. Cells were
586 then centrifuged at 500 *g* for 5 min at 4°C and washed in FACS buffer (2% FBS and
587 0.2 mM ethylenediaminetetraacetic acid (EDTA) in PBS (Gibco, Thermo Fisher
588 Scientific)). Following which, cells were analyzed using the BD LSRFortessa X-20 Cell
589 Analyzer (Becton Dickinson). The samples were initially gated side scatter area (SSC-
590 A) by forward scatter area (FSC-A) to select the RAW264.7 populations. The
591 RAW264.7 population was subsequently gated forward scatter width (FSC-W) by
592 SSC-A to remove doublet populations. The resulting single-cell population was then
593 assessed for CD14 and TLR2 fluorescent marker. Data was calculated relative to
594 uninfected untreated cells which were set as 100% levels for the examined receptors.
595
596 **siRNA transfection**

597 Silencer select pre-designed siRNA (Thermo Fisher Scientific) against *Slc16a1 (Mct-*
598 *1)*, *Hcar1 (Gpr81), Gpr65 and Gapdh* were used. RAW264.7 cells were seeded at 40%
599 density the day before transfection in 6-well plates, and siRNA transfections were
600 performed with Silencer™ siRNA Transfection II Kit (Invitrogen) according to the
601 manufacturer's instructions. Cells were used for experiments after 48 h and also
602 harvested at the same time point after transfection to verify successful gene silencing
603 by RT-PCR.
604
605 **Collection of bacteria cell-free culture supernatants**
606 Bacteria were grown in cell culture media for 6 h, and bacteria-free culture
607 supernatants were collected after centrifugation (6,000 *g*) followed by filtration (using
608 a 0.2 μm syringe filter). Alternatively, supernatants were collected after infecting
609 macrophages with bacteria at various MOIs and then filtered by using a 0.2 μm syringe
610 filter. Sterility of bacteria-free culture supernatants were verified by the absence of
611 viable bacteria when plated on BHI agar.
612
613 **NF-κB reporter assay**
614 Post-infection, 20 μL of supernatant was added to 180 μL of QUANTI-Blue reagent
615 (Invivogen) and incubated overnight at 37 ˚C. SEAP levels were determined at 640 nm
616 using a TECAN M200 microplate reader. All experiments were performed in biological
617 triplicate.
618
619 **Cell viability assay**
620 Simultaneously with supernatant collection for SEAP determination, culture
621 supernatants were collected from each well to measure lactate dehydrogenase (LDH)

622 release, using an LDH cytotoxicity assay (Clontech) according to manufacturer's
623 instructions. Background LDH activity was determined using mock (PBS) treated RAW
624 264.7 cells. Maximal LDH activity was determined by lysing cells with 1% Triton-X.
625 Each condition was assayed in triplicate. Percentage cytotoxicity was calculated as
626 follows: (sample absorbance-background absorbance)/(maximal absorbance-
627 background absorbance) x 100.
628
629 **Transposon library screen**
630 The transposon library was kindly provided by Professor Dunny Gary [90]. To screen
631 the library, the mutants were first inoculated into DMEM for 24 h and 20 μL of the
632 bacteria suspension will be transferred to previously seeded RAW 264.7 cells with 180
633 μL fresh DMEM in the presence of 100 ng/mL of LPS in 96 well microtitre plate.
634 Macrophages were stimulated for 6 h before the supernatant was collected and tested
635 with SEAP assay to determine the NF-κB activity. LPS-only group was used as
636 positive control for reporter activity and signals higher than the means of LPS-only
637 group minus 1 standard deviation was considered positive hits and non-suppressing
638 mutants. Growth kinetics of the selected mutants were performed to exclude the
639 mutants that grow poorly in DMEM. In addition, pictures of the overnight cultures were
640 taken to record the acidifying ability of each mutant by phenol red, a color indicator in
641 DMEM.
642
643 Mutants that grew similarly to *E. faecalis* wildtype further underwent a secondary
644 screening, where they were normalized to MOI 100 and infected the RAW 264.7 cells
645 in the presence of LPS. For the secondary screen, wildtype was used as control and
646 signals higher than means of wildtype group plus 2 standard deviations were

647 considered weak-suppressing mutants and validated hits. To measure the acidification
648 ability of the validated hits, 10^8 CFU of bacteria were inoculated into 5 mL of DMEM
649 for indicated time, and the pH value was determined by pH meter.
650

651 **Lactate concentration measurement**

652 Bacteria were grown in DMEM supplemented with 10% FBS for 6 h in the absence of
653 macrophages before collecting the supernatant and storing it at -80°C until
654 assessment by the L-Lactate Assay Kit (Abcam, Cambridge, UK), according to
655 manufacturer's recommendations. All samples were assessed using the same kit lot
656 and at the same time to avoid inter-assay variability. Alternatively, blood gas analysis
657 using abl90 flex series analyser (Radiometer Medical, Singapore) to quantify lactate
658 concentration.
659

660 **IL-6 quantification**

661 Supernatants were collected from RAW 264.7 cells 6 hpi and stored at -80°C until
662 assessment by the ELISA MAX Deluxe Set Mouse IL-6 assay kit (Biolegend, San
663 Diego, USA), according to manufacturer's recommendations. All samples were
664 assessed using the same kit lot and at the same time to avoid inter-assay variability.
665

666 **Cytokine Luminex xMAP analysis**

667 Supernatants were collected from RAW 264.7 cells 6 hpi and stored at -80°C until
668 assessment by the Bio-Plex ProTM mouse cytokine 23-plex assay kit (Bio-Rad
669 Laboratories), according to manufacturer's recommendations. All samples were
670 assessed using the same kit lot and at the same time to avoid inter-assay variability.

671

672 **Mouse model of wound infection**

673 Bacterial cultures, prepared as described above, were used to infect wounds in 7 to 8
674 weeks old, 20 to 23 g female C57BL/6J mice (InVivos, Singapore). Wounds were
675 prepared as previously described [43]. Briefly, mice were anesthetized with isoflurane
676 (3%) and the dorsal hair was trimmed. After trimming, remaining fine hairs were
677 removed by first applying Nair Cream (Church and Dwight Co, Charles Ewing
678 Boulevard, USA) and shaving using a scalpel. Next, the skin was first disinfected using
679 70% ethanol and a 6 mm biopsy punch (Integra Miltex, New York, USA) was used to
680 create a fill-thickness wound and inoculated with bacteria subsequently. Inoculum
681 volumes of 10 µL, containing a bacterial suspension of either single or polymicrobial
682 species prepared in PBS: (i) 10^2 CFU of *E. coli* strain UTI89 with 10^6 CFU *E. faecalis*
683 wildtype, and (ii) 10^2 CFU of *E. coli* strain UTI89 with 10^6 CFU *E. faecalis* Ldh. Single
684 species controls (10^2 CFU of *E. coli* strain UTI89, 10^6 CFU *E. faecalis* OG1RF, or 10^6
685 CFU *E. faecalis* Ldh) were performed alongside polymicrobial infections. The wound
686 site was then sealed with a sterile transparent dressing (Tegaderm 3M, St Paul
687 Minnesota, USA). After 24 h, animals were euthanized by carbon dioxide inhalation
688 and cervical dislocation and a 1 cm by 1 cm squared piece of skin surrounding the
689 wound was excised and homogenized in 1 mL PBS for CFU enumeration by serial
690 dilution on MacConkey agar (Becton, Dickinson and Company, Franklin Lakes, NJ) or
691 BHI agar supplemented with 10 µg/mL colistin (Sigma-Aldrich, St Louis, MO) and 10
692 µg/mL nalidixic acid (BHI-CNA) (Sigma-Aldrich, St Louis, MO) to isolate *E. coli* or *E.*
693 *faecalis*, respectively.

694

695 **RNA extraction**

696 After 6 hpi with *E. faecalis* at various MOIs in the presence or absence of LPS (100
697 ng/mL), cells were washed once with the tissue culture grade 1X PBS (Gibco, Thermo
698 Fisher Scientific, Singapore) prior to RNA extraction. 1 mL of Trizol (Invitrogen,
699 Thermo Fisher, USA) per well and was stored at -80°C until RNA extraction using
700 Direct-zol RNA Miniprep Plus kit (Zymo Research, USA) according to manufacturer's
701 protocol. Briefly, 200 µL of chloroform (Sigma Aldrich, USA) was first added to 1 mL
702 of Trizol extracted samples, mixed vigorously for 2 min and allowed to stand at room
703 temperature for minimum 10 min. The samples were centrifuged at 12,000 *g* for 15
704 min at 4°C and the top layer (aqueous phase) was transferred to 500 µL of ethanol
705 (Fisher Scientific, Canada) before loading into the Zymo-Spin IIICG Column.
706 Subsequently, RNA extraction was performed according to manufacturer's protocol
707 for Direct-zol RNA Miniprep Plus kit. Next, extracted RNA samples were further
708 cleaned and concentrated using RNA Clean & Concentrator-5 (Zymo Research, USA)
709 following the manufacturer's protocol.

710 RNA samples were first screened using TapeStation (Aligent Technologies, USA) to
711 obtain RIN value and concentration. Qubit analysis was also performed to measure
712 the DNA and RNA concentration using Qubit dsDNA HS Assay Kit (Invitrogen, Thermo
713 Fisher Scientific, USA) and Qubit RNA BR Assay Kit (Invitrogen, Thermo Fisher
714 Scientific, USA), before storage at -80°C until sequencing using an Illumina
715 Hiseq®2500 v.2 (Illumina, Singapore), 150 bp paired-end.

716

717 **Protein extraction and western blot analysis**

718 Following infection with *E. faecalis* as described previously, proteins were harvested
719 using 2x Laemmli buffer (Bio-rad, Hercules, CA) containing 50 mM dithiothreitol
720 (Sigma Aldrich, USA) and denatured at 99°C for 10 min. 30 µL of protein samples

721 were loaded and subjected to Sodium Dodecyl Sulfate-Polyacrylamide Gel
722 Electrophoresis (SDS-PAGE) using NuPAGE 4-12% Bis-Tris Gel (Invitrogen, Thermo
723 Fisher Scientific, USA) in 1 x NuPAGE MOPS SDS Running Buffer (Invitrogen,
724 Thermo Fisher Scientific, USA). The protein samples were transferred to
725 polyvinylidene fluoride (PVDF) membrane using iBlot® Gel Transfer Device
726 (Invitrogen, Thermo Fisher Scientific, USA) as per manufacturer's instructions. The
727 PVDF membrane was then blocked using 5% BSA in Tris-buffered saline (20 mM Tris-
728 HCl pH 7.4, 150 mM NaCl) containing 0.1% Tween-20 (Sigma Aldrich, USA) at room
729 temperature for 1 h. Subsequently, primary antibodies such as MyD88, TAK1,
730 phospho-TAK1, IKKα, IKKβ, phospho-IKKα/β, IκBα, phospho- IκBα, p65, phospho-
731 p65, SAPK/JNK, p38 MAPK, phospho-p38, p44/p42 MAPK (ERK1/2), phospho-
732 p44/p42 MAPK, c-Jun, phospho-c-Jun, c-Fos, phospho-cFos and GADPH (Cell
733 Signalling Technology, USA) were used for probing overnight at 4 °C. The membranes
734 were washed with Tris-buffered saline and incubated with 1:3000 diluted anti-rabbit
735 IgG antibodies conjugated with horseradish peroxidase (Invitrogen, Thermo Fisher
736 Scientific, USA) at room temperature for 1 h. Following which, membranes were
737 washed, and proteins were detected using SuperSignal West Femto Maximum
738 Sensitivity Substrate (Invitrogen, Thermo Fisher Scientific, USA) and autoradiography
739 films (Kodak, USA).
740

741 **Transcriptomics analysis**

742 Sequencing data are available at NCBI's BioProject (accession no. GSE188916). The
743 sequencing was performed at the Singapore Centre for Environmental Life Sciences
744 Engineering High Throughput Sequencing Unit, NTU, Singapore. Following quality
745 control (FastQC v0.11.9), trimming (cutadapt v4.2) and pre-processing using

746 TrimGalore (v0.6.6), the reads were mapped to the Gencode Mouse Release M32
747 (GRCm39) using Salmon (v.1.10.0). Differentially expressed gene analysis was
748 conducted in DESeq2 (v1.38.3) from raw counts. For over-representation and gene
749 set enrichment analysis (GSEA), we utilised clusterProfiler (v 4.6.0), enrichplot (v
750 1.18.3) and DOSE (v 3.24.2) packages for Gene Ontology (GO) analyses. The
751 workflow can be found at https://github.com/cenk-celik/Tien_et_al.

752

753 **Statistical Analysis**

754 Statistical analysis was performed utilizing GraphPad Prism V6 and V10.4.1 software
755 (GraphPad Software, La Jolla, CA). One-way ANOVA (Analysis of Variance) were
756 used to compare between median and the different conditions. Statistical significance
757 for multiplex immunoassay was determined using Kruskal-Wallis statistical analysis.
758 CFU titers were compared using the non-parametric Mann-Whitney U test. *P*-values
759 less than 0.05 were deemed significant. Unless otherwise stated, values represented
760 means ± SEM derived from at least 3 independent experiments.

761

762 **Ethics Statement**

763 All animal experiments were performed with approval from the Institutional Animal
764 Care and Use Committee (IACUC) in Nanyang Technological University (NTU),
765 School of Biological Sciences under protocols ARF-SBS/NIE-A18061, A19061 and
766 A24066.

767
768

769 **Funding:** R.A.G.d.S. and part of this work were supported by the National Research
770 Foundation, Prime Minister's Office, Singapore, under its Campus for Research
771 Excellence and Technological Enterprise (CREATE) program, through core funding of
772 the Singapore-MIT Alliance for Research and Technology (SMART) Antimicrobial

Resistance Interdisciplinary Research Group (AMR IRG). This work was also supported by the National Research Foundation and Ministry of Education Singapore under its Research Centre of Excellence Programme (to the Singapore Centre for Environmental Life Sciences Engineering, SCELSE), and by the Singapore Ministry of Education under its Tier 2 program (MOE2019-T2-2-089) awarded to K.A.K. The funders had no role in study design, data collection and analysis, decision to publish, or preparation of the manuscript.

Author contributions: R.A.G.d.S., B.Y.Q.T., and K.A.K. designed the experiments. R.A.G.d.S., B.Y.Q.T., P.H.N.K., A.Z.C.T., and K.K.L.C. performed experiments. R.A.G.d.S., B.Y.Q.T., P.H.N.K., C.C., M.H.I., and G.H. analyzed data. R.A.G.d.S., B.Y.Q.T. and K.A.K. interpreted the results. B.Y.Q.T. and K.A.K. conceived the project. G.T., J.C., and K.A.K. supervised, acquired funding, and provided resources. R.A.G.d.S., B.Y.Q.T. and K.A.K. wrote the manuscript. All authors reviewed and approved the final manuscript.

Reference

1. Gilmore, M.S., et al., *Enterococci: From commensals to leading causes of drug resistant infection*. 2014, Boston: Massachusetts Eye and Ear Infirmary. .
2. Arias, C.A. and B.E. Murray, *The rise of the Enterococcus: beyond vancomycin resistance.* Nat Rev Microbiol, 2012. **10**(4): p. 266-78.
3. Schmidt-Hieber, M., et al., *Intensified strategies to control vancomycin-resistant enterococci in immunocompromised patients.* Int J Hematol, 2007. **86**(2): p. 158-62.
4. Hidron, A.I., et al., *NHSN annual update: antimicrobial-resistant pathogens associated with healthcare-associated infections: annual summary of data reported to the National Healthcare Safety Network at the Centers for Disease Control and Prevention, 2006-2007.* Infect Control Hosp Epidemiol, 2008. **29**(11): p. 996-1011.
5. Sievert, D.M., et al., *Antimicrobial-resistant pathogens associated with healthcare-associated infections: summary of data reported to the National Healthcare Safety Network at the Centers for Disease Control and Prevention, 2009-2010.* Infect Control Hosp Epidemiol, 2013. **34**(1): p. 1-14.
6. Dombrádi, Z., et al., *A case report of vancomycin-resistant Enterococcus faecalis colonization of a femoral wound in central europe*, in *Open Medicine*. 2009. p. 259.
7. Hollenbeck, B.L. and L.B. Rice, *Intrinsic and acquired resistance mechanisms in enterococcus.* Virulence, 2012. **3**(5): p. 421-33.
8. Archambaud, C., et al., *Enterococcus faecalis: an overlooked cell invader.* Microbiol Mol Biol Rev, 2024. **88**(3): p. e0006924.
9. da Silva, R.A.G., et al., *Enterococcus faecalis alters endo-lysosomal trafficking to replicate and persist within mammalian cells.* PLoS Pathog, 2022. **18**(4): p. e1010434.
10. Oeckinghaus, A., M.S. Hayden, and S. Ghosh, *Crosstalk in NF-kappaB signaling pathways.* Nat Immunol, 2011. **12**(8): p. 695-708.
11. Tato, C.M. and C.A. Hunter, *Host-pathogen interactions: subversion and utilization of the NF-kappa B pathway during infection.* Infect Immun, 2002. **70**(7): p. 3311-7.
12. Oeckinghaus, A. and S. Ghosh, *The NF-kappaB family of transcription factors and its regulation.* Cold Spring Harb Perspect Biol, 2009. **1**(4): p. a000034.
13. Li, D. and M. Wu, *Pattern recognition receptors in health and diseases.* Signal Transduct Target Ther, 2021. **6**(1): p. 291.
14. Baldassarri, L., et al., *Glycosaminoglycans mediate invasion and survival of Enterococcus faecalis into macrophages.* J Infect Dis, 2005. **191**(8): p. 1253-62.
15. Gentry-Weeks, C.R., et al., *Survival of Enterococcus faecalis in mouse peritoneal macrophages.* Infection and Immunity, 1999. **67**(5): p. 2160-2165.
16. Rakita, R.M., et al., *Enterococcus faecalis bearing aggregation substance is resistant to killing by human neutrophils despite phagocytosis and neutrophil activation.* Infect Immun, 1999. **67**(11): p. 6067-75.
17. Roilides, E., et al., *How Biofilms Evade Host Defenses.* Microbiol Spectr, 2015. **3**(3).
18. Zou, J. and N. Shankar, *Enterococcus faecalis infection activates phosphatidylinositol 3-kinase signaling to block apoptotic cell death in macrophages.* Infect Immun, 2014. **82**(12): p. 5132-42.
19. Zou, J. and N. Shankar, *The opportunistic pathogen Enterococcus faecalis resists phagosome acidification and autophagy to promote intracellular survival in macrophages.* Cellular Microbiology, 2016. **18**(6): p. 831-843.
20. Wang, S., et al., *Enterococcus faecalis from healthy infants modulates inflammation through MAPK signaling pathways.* PLoS One, 2014. **9**(5): p. e97523.

838 21. Wang, S., et al., *Infant intestinal Enterococcus faecalis down-regulates inflammatory*
839 *responses in human intestinal cell lines.* World journal of gastroenterology : WJG,
840 2008. **14**(7): p. 1067-76.
841 22. Tien, B.Y.Q., et al., *Enterococcus faecalis Promotes Innate Immune Suppression and*
842 *Polymicrobial Catheter-Associated Urinary Tract Infection.* Infection and immunity,
843 2017. **85**(12): p. e00378-17.
844 23. Zanoni, I., et al., *CD14 controls the LPS-induced endocytosis of Toll-like receptor 4.*
845 Cell, 2011. **147**(4): p. 868-80.
846 24. Kristich, C.J., et al., *Development and use of an efficient system for random mariner*
847 *transposon mutagenesis to identify novel genetic determinants of biofilm formation in*
848 *the core Enterococcus faecalis genome.* Appl Environ Microbiol, 2008. **74**(11): p.
849 3377-86.
850 25. Jönsson, M., et al., *Construction and characterization of three lactate dehydrogenase-*
851 *negative Enterococcus faecalis V583 mutants.* Applied and environmental
852 microbiology, 2009. **75**(14): p. 4901-4903.
853 26. Rana, N.F., et al., *Redox Balance via Lactate Dehydrogenase Is Important for*
854 *Multiple Stress Resistance and Virulence in Enterococcus faecalis.* Infection and
855 Immunity, 2013. **81**(8): p. 2662.
856 27. Harold, F.M. and E. Levin, *Lactic acid translocation: terminal step in glycolysis by*
857 *Streptococcus faecalis.* J Bacteriol, 1974. **117**(3): p. 1141-8.
858 28. Mehmeti, I., et al., *Transcriptome, proteome, and metabolite analyses of a lactate*
859 *dehydrogenase-negative mutant of Enterococcus faecalis V583.* Applied and
860 environmental microbiology, 2011. **77**(7): p. 2406-2413.
861 29. Heming, T.A., et al., *Post-transcriptional effects of extracellular pH on tumour*
862 *necrosis factor-alpha production in RAW 246.7 and J774 A.1 cells.* Clin Sci (Lond),
863 2001. **100**(3): p. 259-66.
864 30. Gentry-Weeks, C.R., et al., *Survival of Enterococcus faecalis in mouse peritoneal*
865 *macrophages.* Infect Immun, 1999. **67**(5): p. 2160-5.
866 31. Mondello, P., et al., *Panobinostat acts synergistically with ibrutinib in diffuse large B*
867 *cell lymphoma cells with MyD88 L265P mutations.* JCI Insight, 2017. **2**(6): p. e90196.
868 32. Rebe, C., et al., *STAT3 activation: A key factor in tumor immunoescape.* JAKSTAT,
869 2013. **2**(1): p. e23010.
870 33. Lee, H.K., et al., *Extracellular Signal-regulated Kinase Activation Is Required for*
871 *Serine 727 Phosphorylation of STAT3 in Schwann Cells in vitro and in vivo.* Korean J
872 Physiol Pharmacol, 2009. **13**(3): p. 161-8.
873 34. Chung, J., et al., *STAT3 serine phosphorylation by ERK-dependent and -independent*
874 *pathways negatively modulates its tyrosine phosphorylation.* Mol Cell Biol, 1997.
875 **17**(11): p. 6508-16.
876 35. Chang, F., et al., *Signal transduction mediated by the Ras/Raf/MEK/ERK pathway*
877 *from cytokine receptors to transcription factors: potential targeting for therapeutic*
878 *intervention.* Leukemia, 2003. **17**(7): p. 1263-93.
879 36. Wu, M., et al., *Hepatitis B virus polymerase inhibits the interferon-inducible MyD88*
880 *promoter by blocking nuclear translocation of Stat1.* J Gen Virol, 2007. **88**(Pt 12): p.
881 3260-3269.
882 37. Kloster, M.M., et al., *Hyperactivation of NF-kappaB via the MEK signaling is*
883 *indispensable for the inhibitory effect of cAMP on DNA damage-induced cell death.*
884 Mol Cancer, 2011. **10**: p. 45.
885 38. Certo, M., et al., *Understanding lactate sensing and signalling.* Trends Endocrinol
886 Metab, 2022. **33**(10): p. 722-735.

887 39. Hajjar, S. and X. Zhou, *pH sensing at the intersection of tissue homeostasis and*
888 *inflammation.* Trends Immunol, 2023. **44**(10): p. 807-825.
889 40. Gerlo, S., et al., *Cyclic AMP: a selective modulator of NF-kappaB action.* Cell Mol
890 Life Sci, 2011. **68**(23): p. 3823-41.
891 41. Heim, C.E., et al., *Lactate production by Staphylococcus aureus biofilm inhibits*
892 *HDAC11 to reprogramme the host immune response during persistent infection.*
893 Nature microbiology, 2020. **5**(10): p. 1271-1284.
894 42. Chong, K.K.L., et al., *Enterococcus faecalis Modulates Immune Activation and Slows*
895 *Healing During Wound Infection.* J Infect Dis, 2017. **216**(12): p. 1644-1654.
896 43. Keogh, D., et al., *Enterococcal Metabolite Cues Facilitate Interspecies Niche*
897 *Modulation and Polymicrobial Infection.* Cell Host Microbe, 2016. **20**(4): p. 493-503.
898 44. Weiner, L.M., et al., *Antimicrobial-Resistant Pathogens Associated With Healthcare-*
899 *Associated Infections: Summary of Data Reported to the National Healthcare Safety*
900 *Network at the Centers for Disease Control and Prevention, 2011-2014.* Infect
901 Control Hosp Epidemiol, 2016. **37**(11): p. 1288-1301.
902 45. Zou, J. and N. Shankar, *Roles of TLR/MyD88/MAPK/NF-κB signaling pathways in*
903 *the regulation of phagocytosis and proinflammatory cytokine expression in response*
904 *to E. faecalis infection.* PLoS ONE, 2015. **10**(8): p. e0136947.
905 46. Zou, J., et al., *A TIR domain protein from E. faecalis attenuates MyD88-mediated*
906 *signaling and NF-kappaB activation.* PLoS One, 2014. **9**(11): p. e112010.
907 47. Ramsey, M., A. Hartke, and M. Huycke, *The Physiology and Metabolism of*
908 *Enterococci*, in *Enterococci: From Commensals to Leading Causes of Drug Resistant*
909 *Infection*, M.S. Gilmore, et al., Editors. 2014: Boston.
910 48. Richardson, A.R., S.J. Libby, and F.C. Fang, *A Nitric Oxide–Inducible Lactate*
911 *Dehydrogenase Enables Staphylococcus aureus to Resist Innate*
912 *Immunity.* Science, 2008. **319**(5870): p. 1672.
913 49. Esvaran, M. and P.L. Conway, *Lactobacilli can attenuate inflammation in mouse*
914 *macrophages exposed to polyethylene particles in vitro.* BMC research notes, 2018.
915 **11**(1): p. 567-567.
916 50. Kim, B., O. Shynlova, and S. Lye, *Probiotic Lactobacillus rhamnosus GR-1 is a*
917 *unique prophylactic agent that suppresses infection-induced myometrial cell*
918 *responses.* Scientific reports, 2019. **9**(1): p. 4698-4698.
919 51. Colegio, O.R., et al., *Functional polarization of tumour-associated macrophages by*
920 *tumour-derived lactic acid.* Nature, 2014. **513**(7519): p. 559-563.
921 52. Dietl, K., et al., *Lactic acid and acidification inhibit TNF secretion and glycolysis of*
922 *human monocytes.* J Immunol, 2010. **184**(3): p. 1200-9.
923 53. Husain, Z., et al., *Tumor-Derived Lactate Modifies Antitumor Immune Response:*
924 *Effect on Myeloid-Derived Suppressor Cells and NK Cells.* The Journal of
925 Immunology, 2013. **191**(3): p. 1486.
926 54. Morrot, A., et al., *Metabolic Symbiosis and Immunomodulation: How Tumor Cell-*
927 *Derived Lactate May Disturb Innate and Adaptive Immune Responses.* Frontiers in
928 oncology, 2018. **8**: p. 81-81.
929 55. Mu, X., et al., *Tumor-derived lactate induces M2 macrophage polarization via the*
930 *activation of the ERK/STAT3 signaling pathway in breast cancer.* Cell Cycle, 2018.
931 **17**(4): p. 428-438.
932 56. Romero-Garcia, S., et al., *Lactate Contribution to the Tumor Microenvironment:*
933 *Mechanisms, Effects on Immune Cells and Therapeutic Relevance.* Frontiers in
934 immunology, 2016. **7**: p. 52-52.
935 57. Bidani, A., et al., *Evidence for pH sensitivity of tumor necrosis factor-alpha release*
936 *by alveolar macrophages.* Lung, 1998. **176**(2): p. 111-21.

58. Grabowski, J., et al., *Tumor necrosis factor expression is ameliorated after exposure to an acidic environment.* The Journal of surgical research, 2012. **173**(1): p. 127-134.
59. Mogi, C., et al., *Involvement of Proton-Sensing TDAG8 in Extracellular Acidification-Induced Inhibition of Proinflammatory Cytokine Production in Peritoneal Macrophages.* The Journal of Immunology, 2009. **182**(5): p. 3243.
60. Fernandez, S.F., et al., *Low pH Environmental Stress Inhibits LPS and LTA-Stimulated Proinflammatory Cytokine Production in Rat Alveolar Macrophages.* BioMed Research International, 2013. **2013**: p. 742184.
61. Gerry, A.B. and D.S. Leake, *Effect of low extracellular pH on NF-κB activation in macrophages.* Atherosclerosis, 2014. **233**(2): p. 537-544.
62. Shi, W., et al., *Lactic acid induces transcriptional repression of macrophage inflammatory response via histone acetylation.* Cell Rep, 2024. **43**(2): p. 113746.
63. Rao, K.M., *MAP kinase activation in macrophages.* J Leukoc Biol, 2001. **69**(1): p. 3-10.
64. Traves, P.G., et al., *Relevance of the MEK/ERK signaling pathway in the metabolism of activated macrophages: a metabolomic approach.* J Immunol, 2012. **188**(3): p. 1402-10.
65. Rosenberger, C.M. and B.B. Finlay, *Macrophages inhibit Salmonella typhimurium replication through MEK/ERK kinase and phagocyte NADPH oxidase activities.* J Biol Chem, 2002. **277**(21): p. 18753-62.
66. Panagi, I. and T.L. Thurston, *Ready, STAT3, Go! Bacteria in the race for M2 macrophage polarisation.* Curr Opin Microbiol, 2023. **73**: p. 102285.
67. Hwang, J.T., et al., *Lactococcus lactis KR-050L inhibit IL-6/STAT3 activation.* J Appl Microbiol, 2017. **122**(5): p. 1412-1422.
68. Casey, J.R., S. Grinstein, and J. Orlowski, *Sensors and regulators of intracellular pH.* Nat Rev Mol Cell Biol, 2010. **11**(1): p. 50-61.
69. Balgi, A.D., et al., *Regulation of mTORC1 signaling by pH.* PLoS One, 2011. **6**(6): p. e21549.
70. Chang, Q., et al., *The IL-6/JAK/Stat3 feed-forward loop drives tumorigenesis and metastasis.* Neoplasia, 2013. **15**(7): p. 848-62.
71. Yang, K., et al., *Lactate Suppresses Macrophage Pro-Inflammatory Response to LPS Stimulation by Inhibition of YAP and NF-kappaB Activation via GPR81-Mediated Signaling.* Front Immunol, 2020. **11**: p. 587913.
72. Heim, C.E., et al., *Lactate production by Staphylococcus aureus biofilm inhibits HDAC11 to reprogramme the host immune response during persistent infection.* Nat Microbiol, 2020. **5**(10): p. 1271-1284.
73. Loike, J.D., et al., *Lactate transport in macrophages.* J Immunol, 1993. **150**(5): p. 1951-8.
74. Nonaka, M., et al., *Lactic acid induces HSPA1A expression through ERK1/2 activation.* Biosci Biotechnol Biochem, 2023. **87**(2): p. 191-196.
75. Falck Miniotis, M., et al., *MEK1/2 inhibition decreases lactate in BRAF-driven human cancer cells.* Cancer Res, 2013. **73**(13): p. 4039-49.
76. Ohno, Y., et al., *Lactate increases myotube diameter via activation of MEK/ERK pathway in C2C12 cells.* Acta Physiol (Oxf), 2018. **223**(2): p. e13042.
77. Xue, L. and J.M. Lucocq, *Low extracellular pH induces activation of ERK 2, JNK, and p38 in A431 and Swiss 3T3 cells.* Biochem Biophys Res Commun, 1997. **241**(2): p. 236-42.
78. Chen, B., et al., *ERK-mediated NF-kappaB activation through ASIC1 in response to acidosis.* Oncogenesis, 2016. **5**(12): p. e279.

79. Hirata, S., et al., *Extracellular acidic environments induce phosphorylation of ZAP-70 in Jurkat T cells.* Immunol Lett, 2008. **115**(2): p. 105-9.
80. Aguirre, M. and M.D. Collins, *Lactic acid bacteria and human clinical infection.* J Appl Bacteriol, 1993. **75**(2): p. 95-107.
81. Rossi, F., et al., *Lactobacilli Infection Case Reports in the Last Three Years and Safety Implications.* Nutrients, 2022. **14**(6).
82. da Silva, R.A.G., et al., *Bosutinib Stimulates Macrophage Survival, Phagocytosis, and Intracellular Killing of Bacteria.* ACS Infect Dis, 2024. **10**(5): p. 1725-1738.
83. da Silva, R.A.G., et al., *Mitoxantrone targets both host and bacteria to overcome vancomycin resistance in Enterococcus faecalis.* Sci Adv, 2023. **9**(8): p. eadd9280.
84. Chen, S.L., et al., *Identification of genes subject to positive selection in uropathogenic strains of Escherichia coli: a comparative genomics approach.* Proceedings of the National Academy of Sciences of the United States of America, 2006. **103**(15): p. 5977-82.
85. Mulvey, M.A., J.D. Schilling, and S.J. Hultgren, *Establishment of a persistent Escherichia coli reservoir during the acute phase of a bladder infection.* Infect Immun, 2001. **69**(7): p. 4572-9.
86. Dunny, G.M., B.L. Brown, and D.B. Clewell, *Induced cell aggregation and mating in Streptococcus faecalis: evidence for a bacterial sex pheromone.* Proc Natl Acad Sci U S A, 1978. **75**(7): p. 3479-83.
87. Paulsen, I.T., et al., *Role of mobile DNA in the evolution of vancomycin-resistant Enterococcus faecalis.* Science, 2003. **299**(5615): p. 2071-4.
88. Weischenfeldt, J. and B. Porse, *Bone Marrow-Derived Macrophages (BMM): Isolation and Applications.* CSH Protoc, 2008. **2008**: p. pdb.prot5080.
89. Pfaffl, M.W., *A new mathematical model for relative quantification in real-time RT-PCR.* Nucleic Acids Res, 2001. **29**(9): p. e45.
90. Kristich, C.J., et al., *Development and use of an efficient system for random mariner transposon mutagenesis to identify novel genetic determinants of biofilm formation in the core Enterococcus faecalis genome.* Applied and environmental microbiology, 2008. **74**(11): p. 3377-3386.

1036 **Figures**

1037

1038

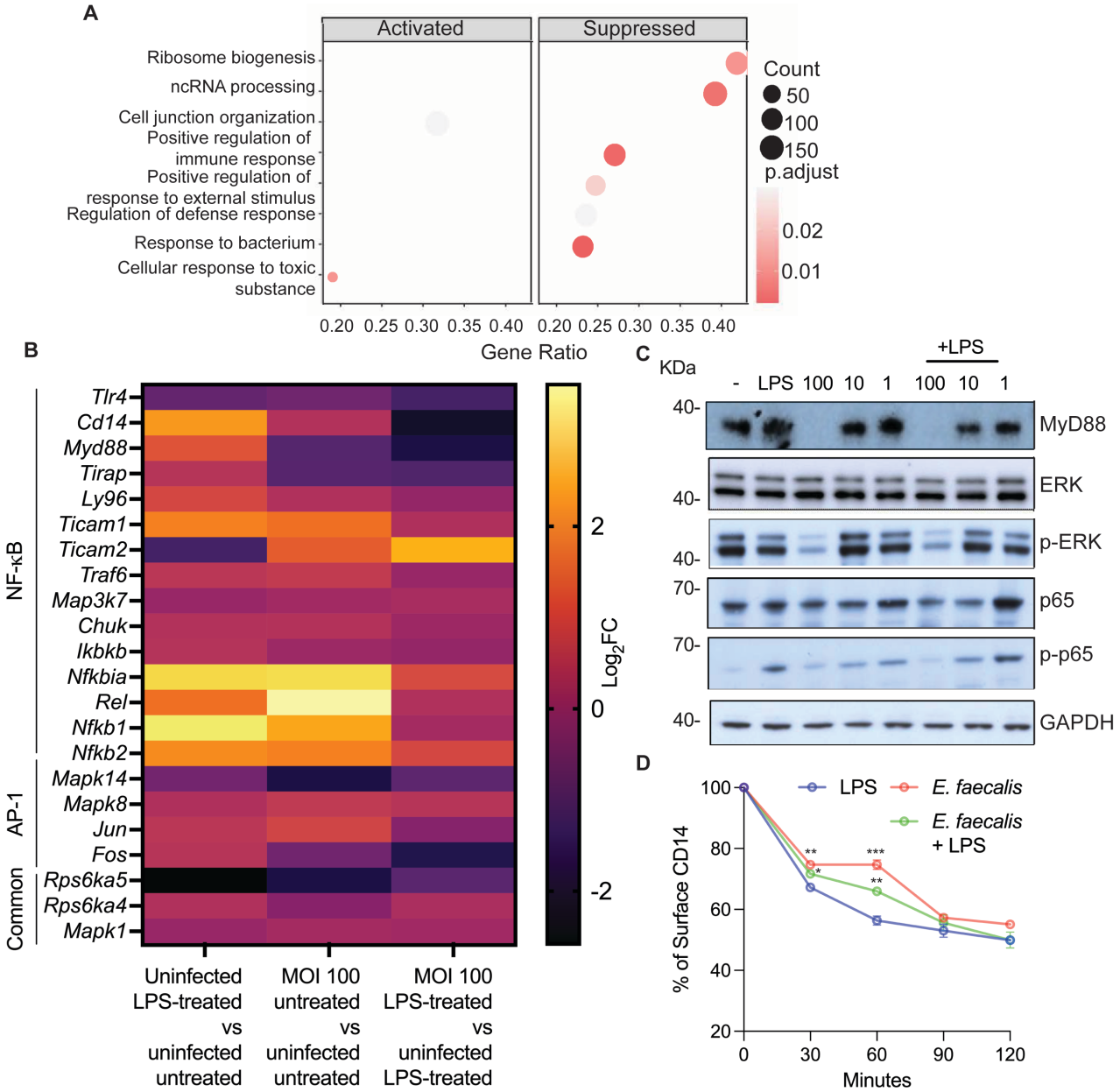

1039

1040

1041

1042 **Figure 1 – *E. faecalis* modulates the macrophage response to bacteria by**

1043 **reducing MyD88 protein levels and preventing ERK and p65 phosphorylation.**

1044 **(A)** GSEA using gene ontology biological process gene sets showing significantly

1045 enriched pathways in RAW 264.7 macrophages infected with *E. faecalis* OG1RF for 6

1046 h at MOI 100 in the presence of LPS (100 ng/mL) compared to uninfected LPS-treated

1047 macrophages. Activated and suppressed pathways were determined based on genes
1048 that are over and under expressed in the analysed pathways. **(B)** Heatmap of
1049 differentially expressed NF-κB/ AP-1-related genes. **(C)** Western blots performed on
1050 protein extracted from RAW 264.7 macrophages infected with *E. faecalis* at the
1051 indicated MOI (100, 10, 1) with or without LPS for 6 h and probed with antibodies
1052 specific for MyD88, ERK, p-ERK, p65, p-p65 and GAPDH. The two bands for ERK
1053 and p-ERK immunoblots represent ERK isoforms 1 and 2. Data shown are
1054 representative of at least 3 independent experiments. **(D)** RAW 264.7 cells were either
1055 infected or treated with LPS alone or in combination for the times indicated before
1056 CD14 endocytosis was examined by flow cytometry. Data (mean ± SEM) are a
1057 summary of three independent experiments and calculated relative to uninfected
1058 untreated cells which were set as 100% levels for the examined receptor. Statistical
1059 analysis was performed using ordinary one-way ANOVA followed by Dunnett's
1060 multiple comparison test *$p<0.05$, **$p<0.01$ and ***$p<0.001$.
1061
1062
1063

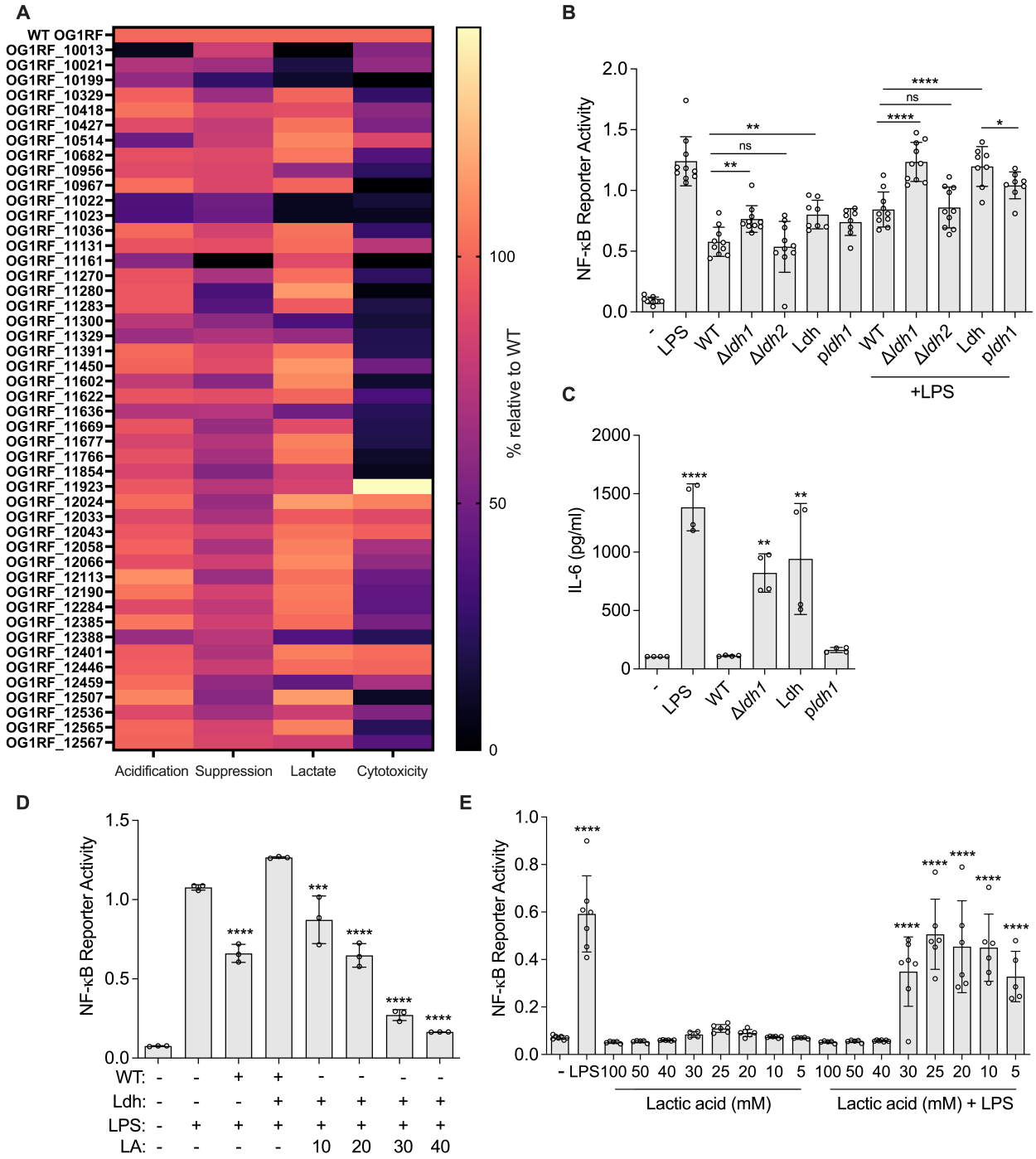

Figure 2 – *E. faecalis* LDH is essential for suppression of NF-κB activation in macrophages.

(A) Bacterial genes identified in a transposon library screen for genes important in macrophage suppression at MOI 100. The heat map shows the degree of NF-κB suppression, medium acidification, lactate production, and cytotoxicity in RAW 264.7 macrophages infected at MOI 100 at 6 hpi relative to WT levels set to 100%. **(B)** RAW

1071 264.7 macrophages were infected with WT, Δ*ldh1,* Δ*ldh2,* Ldh*,* or *ldh1*
1072 complementation strains alone or concurrently with LPS at MOI 100 for 6 h prior to
1073 measurement of NF-κB-driven SEAP reporter activity. **(C)** BMDMs were infected with
1074 Δ*ldh1,* Ldh, or *ldh1* complemented strain for 6 h prior to measurement of IL-6
1075 production. **(D)** RAW 264.7 cells were infected with WT *E. faecalis* or Ldh
1076 supplemented with lactic acid (LA) at various concentration (mM) for 6 h prior to
1077 measurement of NF-κB-driven SEAP reporter activity. **(E)** RAW 264.7 cells were
1078 incubated with cell culture media supplemented with lactic acid at various
1079 concentrations for 6 h prior to measurement of NF-κB-driven SEAP reporter activity.
1080 Data (mean ± SEM) are a summary of at least three independent experiments.
1081 Statistical analysis was performed using one-way ANOVA with Fisher's LSD in **(B)** or
1082 Tukey's multiple comparison test where *$p<0.05$, **$p<0.01$, ***$p<0.001$ and
1083 ****$p<0.001$ as indicated or as compared to media alone for **(C)** and **(E)**, and LPS for
1084 **(D)**.
1085
1086
1087
1088
1089
1090
1091
1092

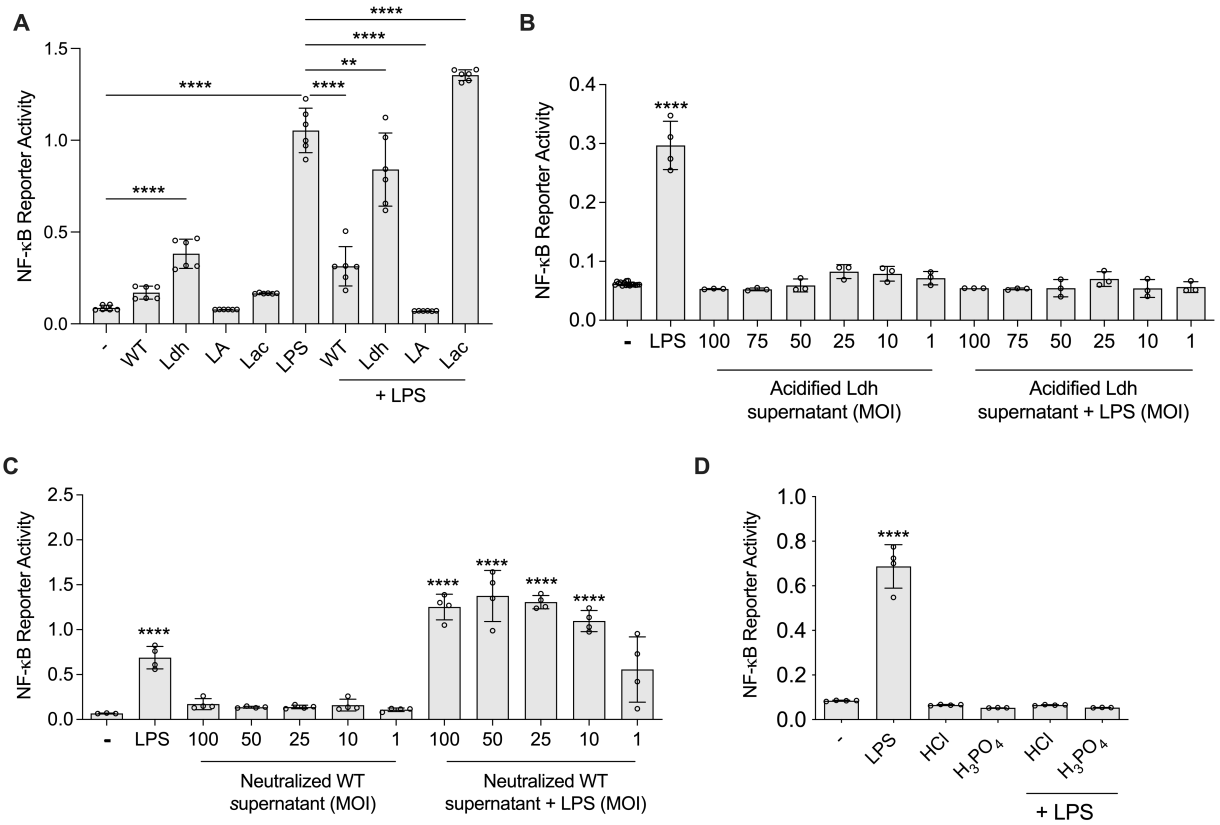

Figure 3 – Acidification is necessary and sufficient for *E. faecalis* suppression of macrophage activation.

(**A**) RAW 264.7 macrophages were infected with WT or Ldh or incubated with cell culture media supplemented with lactic acid or sodium lactate (40 mM) in the presence or absence of LPS for 6 h prior to measurement of NF-κB-driven SEAP reporter activity. RAW 264.7 macrophages were incubated with **(B)** lactic acid-acidified, **(C)** neutralised bacterial-free supernatant (equivalent to shown MOI starting bacterial culture grown for 6 h in cell culture media in the absence of macrophages) and **(D)** HCl and H_3PO_4 acidified media for 6 h prior to measurement of NF-κB-driven SEAP reporter activity. Data (mean ± SEM) are a summary of at least three independent experiments. Statistical analysis was performed using one-way ANOVA with Tukey's multiple comparison tests where NS indicates $p > 0.05$, **$p<0.01$, ***$p<0.001$ and ****$p<0.001$ as compared to media alone unless otherwise indicated.

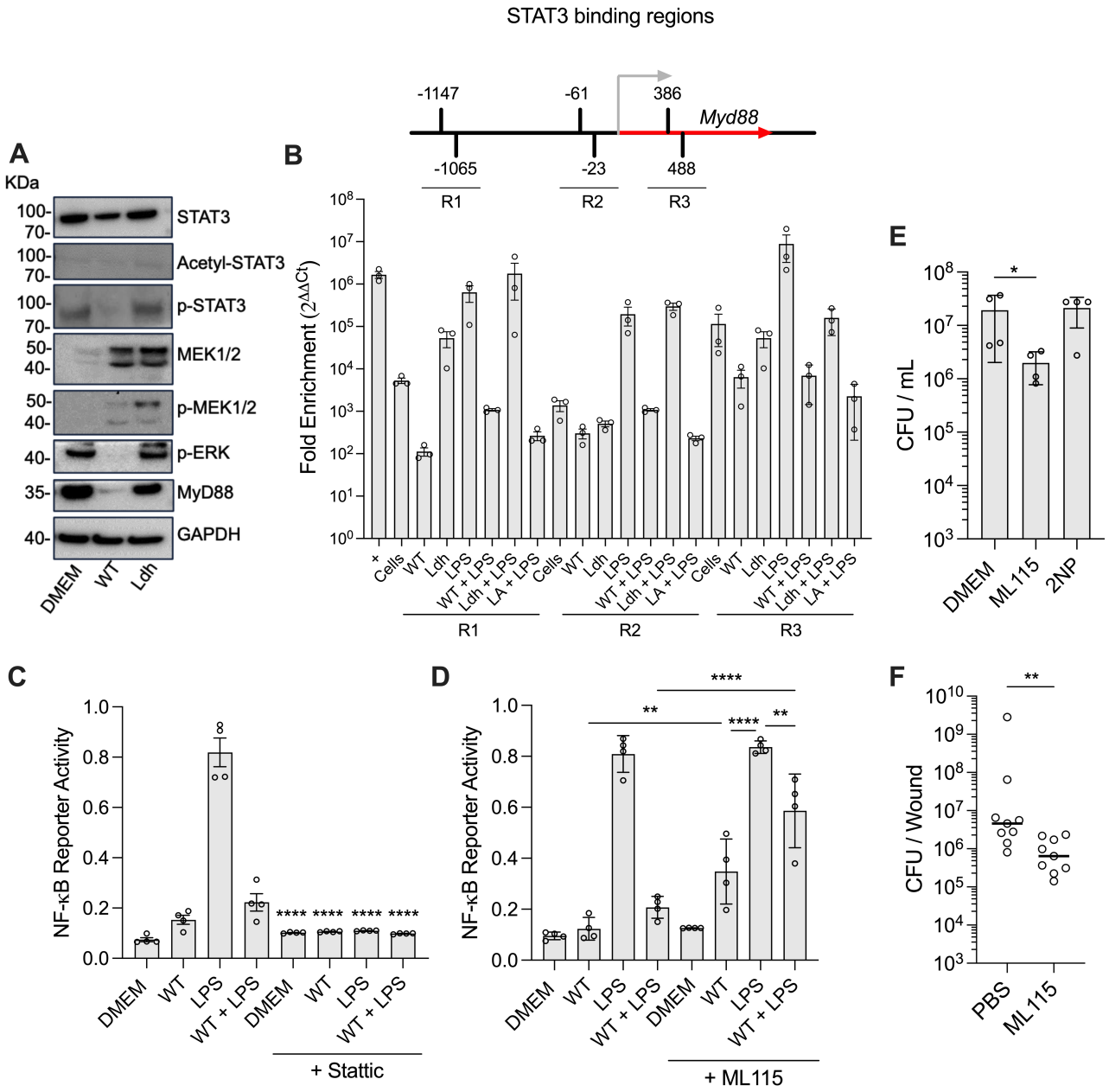

Figure 4 – *E. faecalis* infection reduces MyD88 expression by decreasing STAT3 activity in macrophages. (A) Western blot was performed on protein extracted from RAW 264.7 macrophages WT or Ldh mutant that were incubated for 6 h and probed with antibodies raised against STAT3, acetyl-STAT3, p-STAT3, MEK1/2, p-MEK1/2, p-ERK, MyD88 and GAPDH. **(B)** ChIP–qPCR for STAT3 of the three regions associated with the MyD88 transcriptional starting site in purified DNA of RAW 264.7

1118 cells that were infected with WT or Ldh strains with or without LPS treatment for 6 h.
1119 Treatment with LA in the presence of LPS was also included. A depiction of these
1120 regions relative to the transcriptional starting site (gray arrow) of *Myd88* is shown. The
1121 positive control was established for an RNA polymerase binding site for the *Gapdh*
1122 gene. Replicates from 3 independent experiments are shown. RAW 264.7
1123 macrophages were infected with the WT strain and incubated with cell culture media
1124 in presence or absence of LPS and **(C)** Stattic (10 μM) and **(D)** ML115 (1 μM) for 6 h
1125 prior to measurement of NF-κB-driven SEAP reporter activity. Stattic and ML115 were
1126 added 30 min before the beginning of the experiment. Data (mean ± SEM) are a
1127 summary of at least three independent experiments. Statistical analysis was
1128 performed using one-way ANOVA with Tukey's multiple comparison tests where ns,
1129 $p > 0.05$, **$p<0.01$, ***$p<0.001$ and ****$p<0.001$ as compared to LPS unless otherwise
1130 indicated. **(E)** RAW264.7 cells were infected with *E. faecalis* for 3 h, followed by 1 h of
1131 antibiotic treatment to kill extracellular bacteria. The antibiotic-containing medium was
1132 removed, cells were washed, and a new solution with antibiotics was added together
1133 with ML115 (1 μM) and 2NP (45 μM). Viable intracellular CFU were enumerated after
1134 18 h incubation. Data (mean ± SEM) are a summary of at least three independent
1135 experiments. Statistical analysis was performed using ordinary one-way ANOVA
1136 followed by Tukey's multiple comparison test ns, $p>0.05$; *$p\leq0.05$. **(F)** Using a murine
1137 wound model, mice were infected with 10^6 CFU of WT *E. faecalis* and CFU were
1138 enumerated at 24 hpi after treatment with either PBS or 10 μL of ML115 (100 μM).
1139 Each symbol represents one mouse with the median indicated by the horizontal line.
1140 Data are from at least 2 independent experiments with three to five mice per
1141 experiment. Statistical analysis was performed using the nonparametric Mann-
1142 Whitney test to compare ranks; **$p<0.01$.

1143

1144
1145

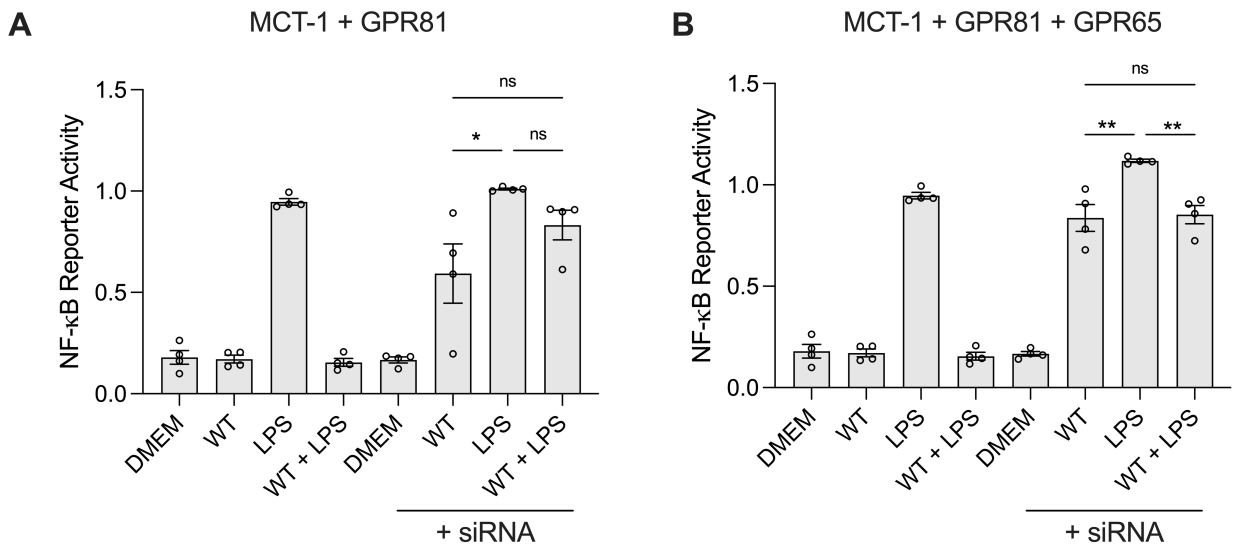

1146
1147 **Figure 5 – The pH-sensitive lactate transporter MCT-1 and lactate sensor GPR81**

1148 **mediate the suppression of NF-κB by *E. faecalis*.** RAW 264.7 macrophages, with

1149 or without siRNA silenced lactate transporters and sensors, were infected with the

1150 OG1RF and incubated with cell culture media in the presence or absence of LPS for

1151 6 h prior to measurement of NF-κB-driven SEAP reporter activity. Silencing the

1152 expression of *Mct-1* + *Gpr81* or *Mct-1* + *Gpr81* + *Gpr65* was achieved by siRNA. Data

1153 (mean ± SEM) represent three independent experiments. Statistical analysis was

1154 performed using ordinary one-way ANOVA followed by Tukey's multiple comparison

1155 test ns, $p>0.05$; *$p\leq0.05$; and **$p<0.01$.

1156
1157

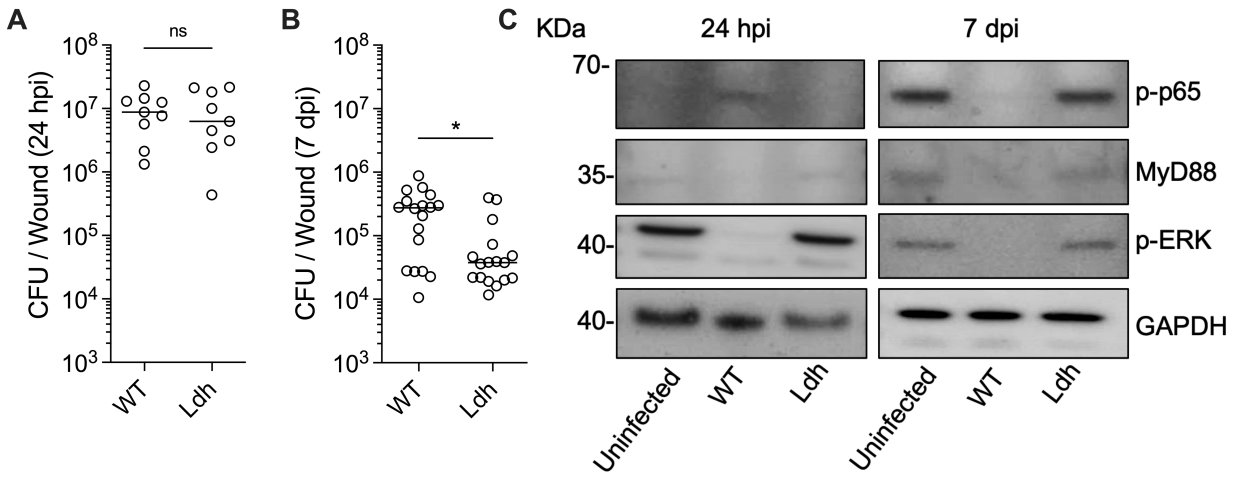

Figure 6 – *E. faecalis* LDH activity contributes to persistence in the wound. (A) Using a wound model, mice were infected with 10^6 CFU each of WT or Ldh mutant and CFU were enumerated at 24 hpi and 7 dpi. Each symbol represents one mouse with the median indicated by the horizontal line. Data are from at least 2 independent experiments with three to five mice per experiment. Statistical analysis was performed using the nonparametric Mann-Whitney test to compare ranks; ns, p>0.05, *p≤0.05. **(B)** Western blot performed on protein extracted from harvested wound lysates of WT or Ldh infections 24 hpi or 7 dpi and probed with antibodies raised against p-p65, MyD88, p-ERK and GAPDH.

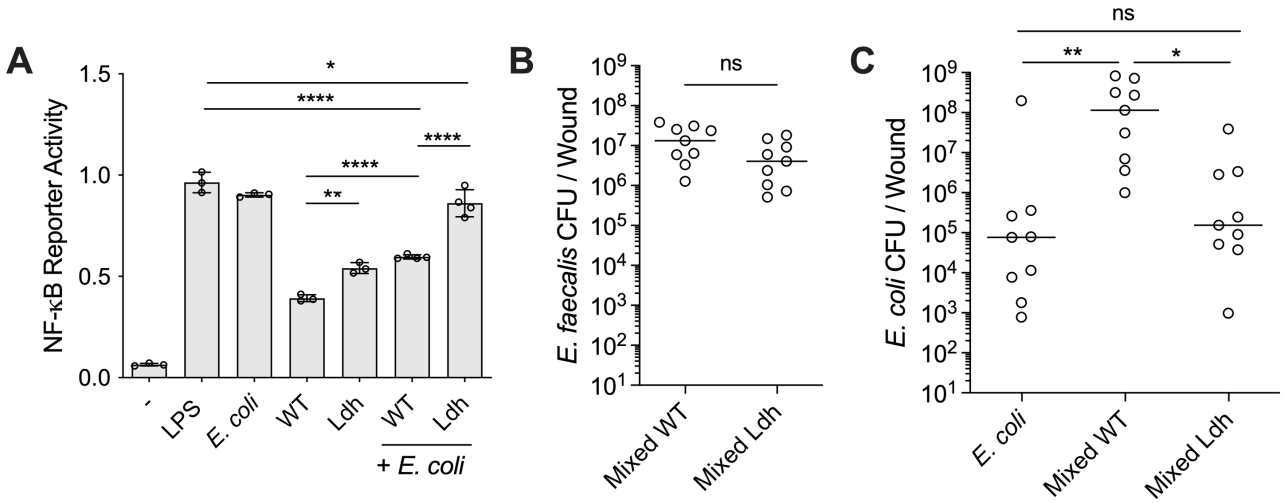

1172 **Figure 7 – *E. faecalis* LDH-mediated immune suppression promotes *E. coli***
1173 **growth during polymicrobial infection.**
1174 (**A**) RAW 264.7 macrophages were infected with *E. coli* strain UTI89 at MOI 0.125,
1175 WT *E. faecalis* or Ldh mutant at MOI 100 in single species control or mixed species
1176 infection for 6 h prior to measurement of NF-κB-driven SEAP reporter activity. Data
1177 (mean ± SEM) are summary from at least 3 independent experiment. Statistical
1178 analysis was performed using ordinary one-way ANOVA, followed by Tukey's multiple
1179 comparison test; ns, $p>0.05$; ***$p\leq 0.001$; and ****$p\leq 0.0001$. Using a wound model,
1180 mice were infected with 10^2 CFU/wound *E. coli* UTI89 or 10^6 CFU each of WT *E.*
1181 *faecalis* or Ldh mutant in single-species control for UTI89 or mixed species infections.
1182 24 hpi CFU enumeration was performed for **(B)** *E. faecalis* and **(C)** *E. coli*. Each
1183 symbol represents one mouse with the median indicated by the horizontal line. Data
1184 are from at least 2 independent experiments with four to five mice per experiment.
1185 Statistical analysis was performed using the nonparametric Mann-Whitney test to
1186 compare ranks **(B)** and using Kruskal-Wallis test with Dunn's posttest **(C)**; ns, $p>0.05$;
1187 *$p\leq 0.05$; and **$p\leq 0.01$.
1188

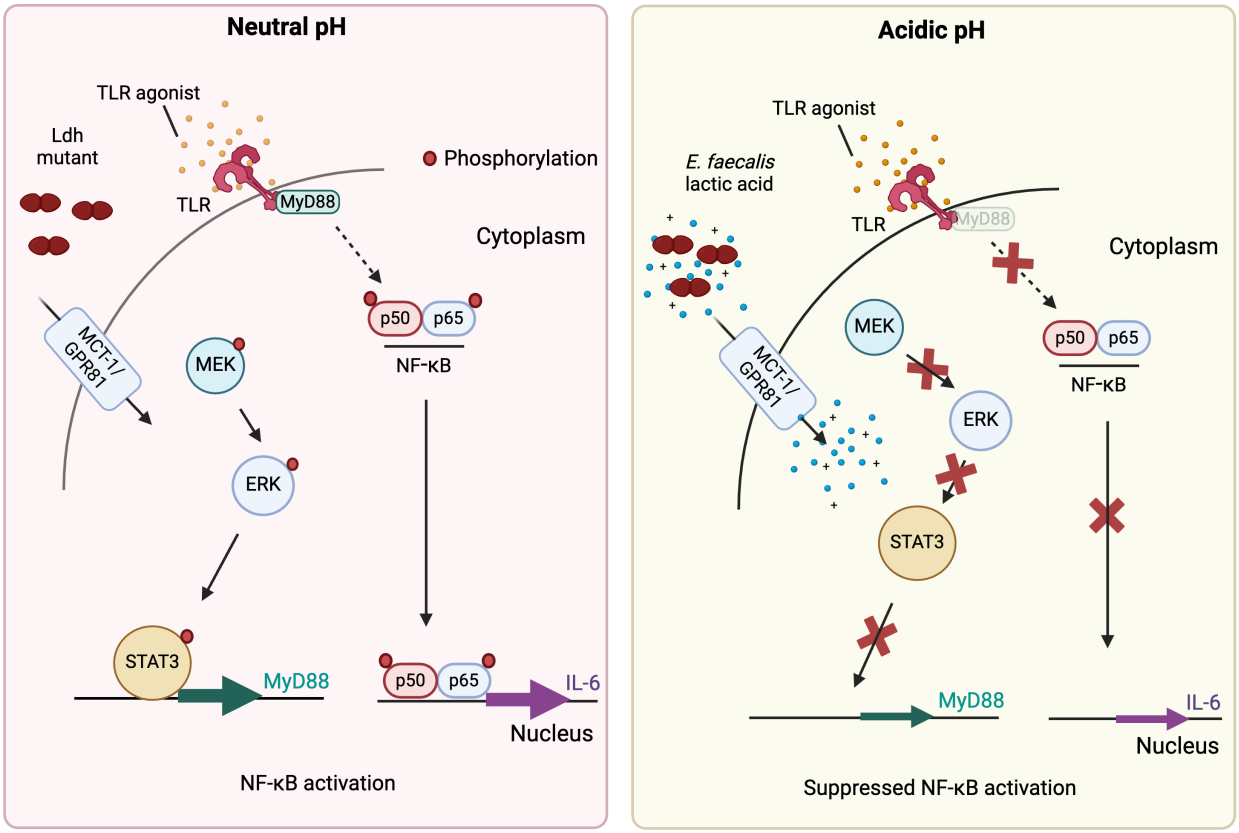

Figure 8 – Model for *E. faecalis*-derived lactic acid suppression of NF-κB activation.

TLR receptors in macrophages sense agonists to trigger NF-κB activation mediated by MyD88. *E. faecalis*-derived lactic acid leads to acidic pH, which contributes to the decrease of the phosphorylation of proteins involved in STAT3 activation and, consequently, *Myd88* expression. The low abundance of MyD88 will prevent MyD88-dependent TLR signaling and, ultimately, NF-κB activation. Created with BioRender.com.

1202 **Supplementary Figures**

1203

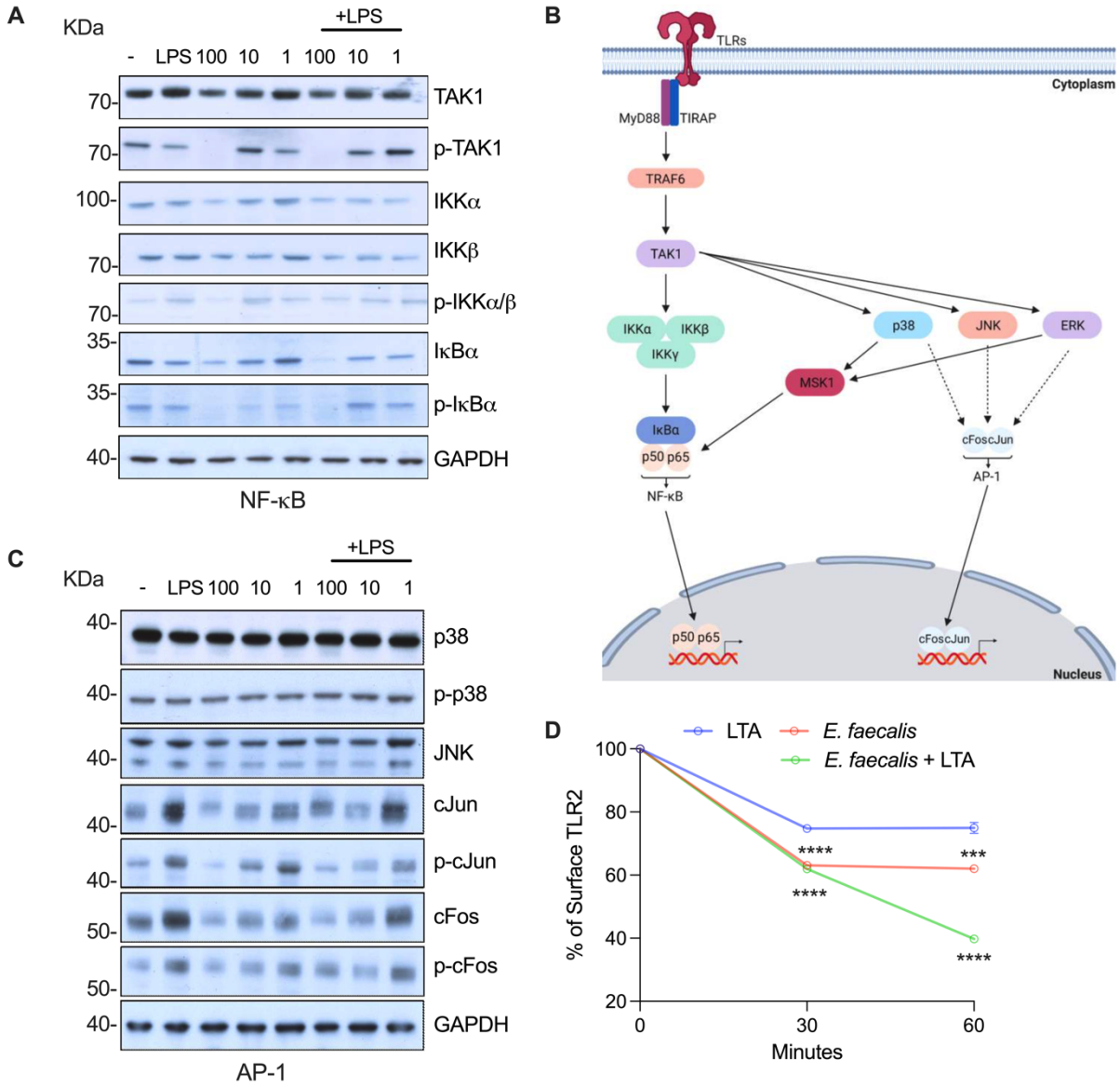

1204

1205 **Figure S1 – *E. faecalis* infection modulates macrophage response to bacteria by**

1206 **affecting the production and phosphorylation status of different proteins of the**

1207 **NF-κB pathway.**

1208 **(A)** Western blot performed on protein extracted from RAW 264.7 macrophages

1209 infected with WT *E. faecalis* at the indicated MOI (100, 10, 1) with or without LPS (100

1210 ng/mL) for 6 h and probed with antibodies specific for TAK1, phospho-TAK1, IKKα,

1211 IKKβ, phospho-IKKα/β, IκBα, phospho-IκBα, p65, phospho-p65 and GAPDH. M

1212 represents uninfected macrophages. GAPDH was used as an internal control for

1213 loading control. **(B)** TLR-NF-κB signaling pathway and cross-talk between NF-κB and
1214 AP-1 are shown. **(C)** Western blot performed on protein extracted from RAW 264.7
1215 macrophages infected with wildtype *E. faecalis* at the indicated MOIs (100, 10, 1) with
1216 or without LPS for 6 h and probed with antibodies specific for p38, phospho-p38, JNK,
1217 ERK, c-Jun, phospho c-Jun, c-Fos, phospho c-Fos and GAPDH. **(D)** RAW 264.7 cells
1218 were either infected or treated with LTA (10 μg/mL) for the times indicated before TLR2
1219 endocytosis was examined by flow cytometry. Data (mean ± SEM) are a summary of
1220 three independent experiments and calculated relative to uninfected untreated cells
1221 which were set as 100% levels for the examined receptor. Statistical analysis was
1222 performed using ordinary one-way ANOVA followed by Dunnett's multiple comparison
1223 test ***$p<0.001$ and ****$p<0.001$.
1224
1225
1226
1227
1228

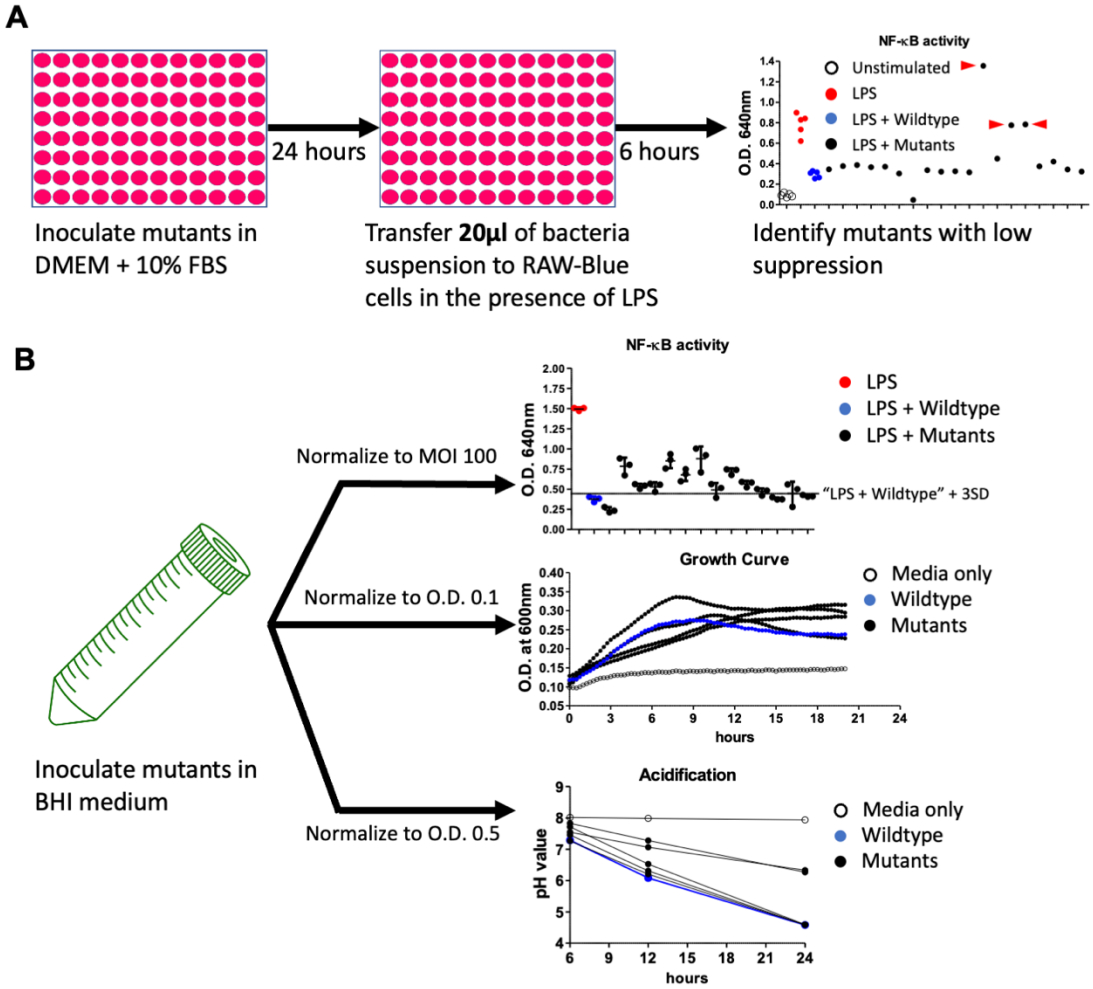

Figure S2 – Methodology for transposon library screen to identify bacterial factor(s) important in macrophage suppression.

(A) Primary screening workflow: all mutants were inoculated in DMEM + 10% FBS for 24 h before 20 µL of the bacteria suspension was transferred to RAW 264.7 cell culture. The macrophages were stimulated in the presence of LPS for 6 h and supernatant was collected for SEAP assay. Mutants showed significant higher NF-κB activity were identified as weak-suppressing mutants. **(B)** Secondary screening: the shortlisted mutants were grown in BHI overnight (16 h) and normalized to indicated concentration and tested for suppressing effect, growth, and acidifying ability in DMEM + 10% FBS.

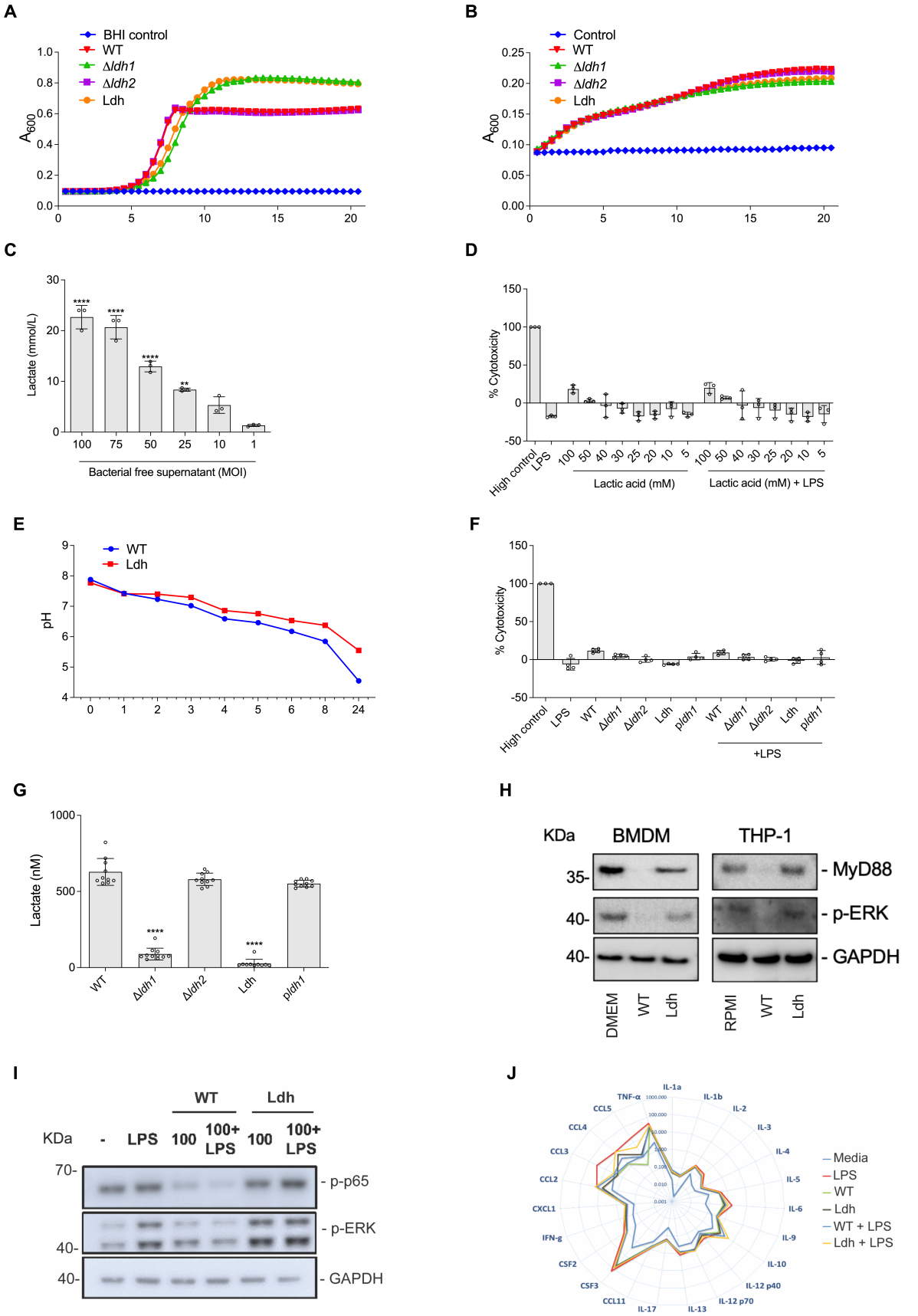

Figure S3 – LDH mutant does not have growth defects and acidifies the environment weakly.

1244 Growth curve for *E. faecalis* strains grown overnight in either **(A)** BHI or **(B)** cell culture
1245 media supplemented with 10% FBS. **(C)** Lactate present in bacterial-free supernatant
1246 was quantified via blood gas analysis. **(D)** RAW 264.7 macrophages was incubated
1247 with cell culture media supplemented with lactate at various concentrations for 6 h
1248 prior to measurement of LDH activity to measure cytotoxicity. **(E)** pH for *E. faecalis*
1249 strains grown in cell culture media measured over a time course. **(F)** RAW 264.7
1250 macrophages infected with WT OG1RF or Ldh mutant supplemented with lactic acid
1251 at various concentration for 6 h prior to measurement of LDH activity. **(G)** Lactate
1252 concentration was measured using 6 hpi bacterial free supernatant. Western blot
1253 performed on protein extracted from BMDMs, THP-1s and RAW 264.7 macrophages
1254 infected with *E. faecalis* MOI 100 for 6 h and probed with antibodies specific for **(H)**
1255 MyD88, p-ERK and GAPDH, and **(I)** p-p65, p-ERK and GAPDH. Samples in **(H)** are
1256 with or without LPS. Data (mean ± SEM) are a summary of at least three independent
1257 experiments. **(J)** Spider plot showing the fold changes of cytokines, chemokines, and
1258 growth factors detected in filtered supernatants collected at 6 hpi for WT *E. faecalis*
1259 and Ldh mutant after normalization against the medium control. Statistical analysis
1260 was performed using one-way ANOVA with Tukey's multiple comparison test where
1261 ****$P<0.0001$ among all the different *E. faecalis* strains as compared to wildtype.

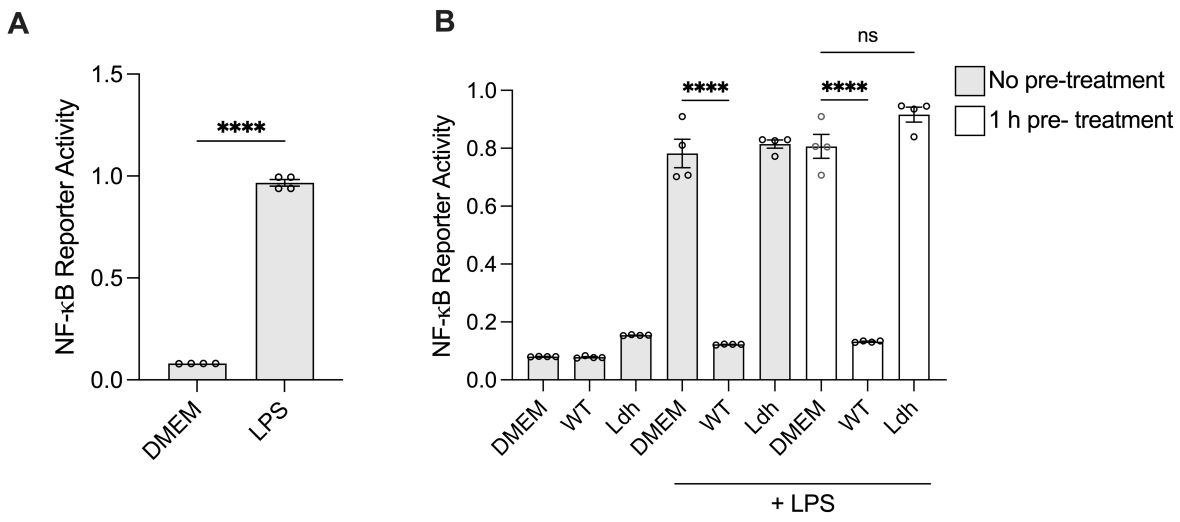

Figure S4 – *E. faecalis* suppresses NF-κB activation in LPS pre-treated cells. **(A)** RAW 264.7 cells were pre-treated for 1 h with LPS prior to measurement of NF-κB-driven SEAP reporter activity. **(B)** RAW 264.7 cells infected with WT *E. faecalis* or Ldh mutant for 6 h prior to measurement of NF-κB-driven SEAP reporter activity were either pre-treated or not with LPS for 1 h prior to infection. Data (mean ± SEM) are a summary of at least three independent experiments. Statistical analysis was performed using one-way ANOVA with Tukey's multiple comparison test where NS, $p>0.05$ and ****$p<0.001$

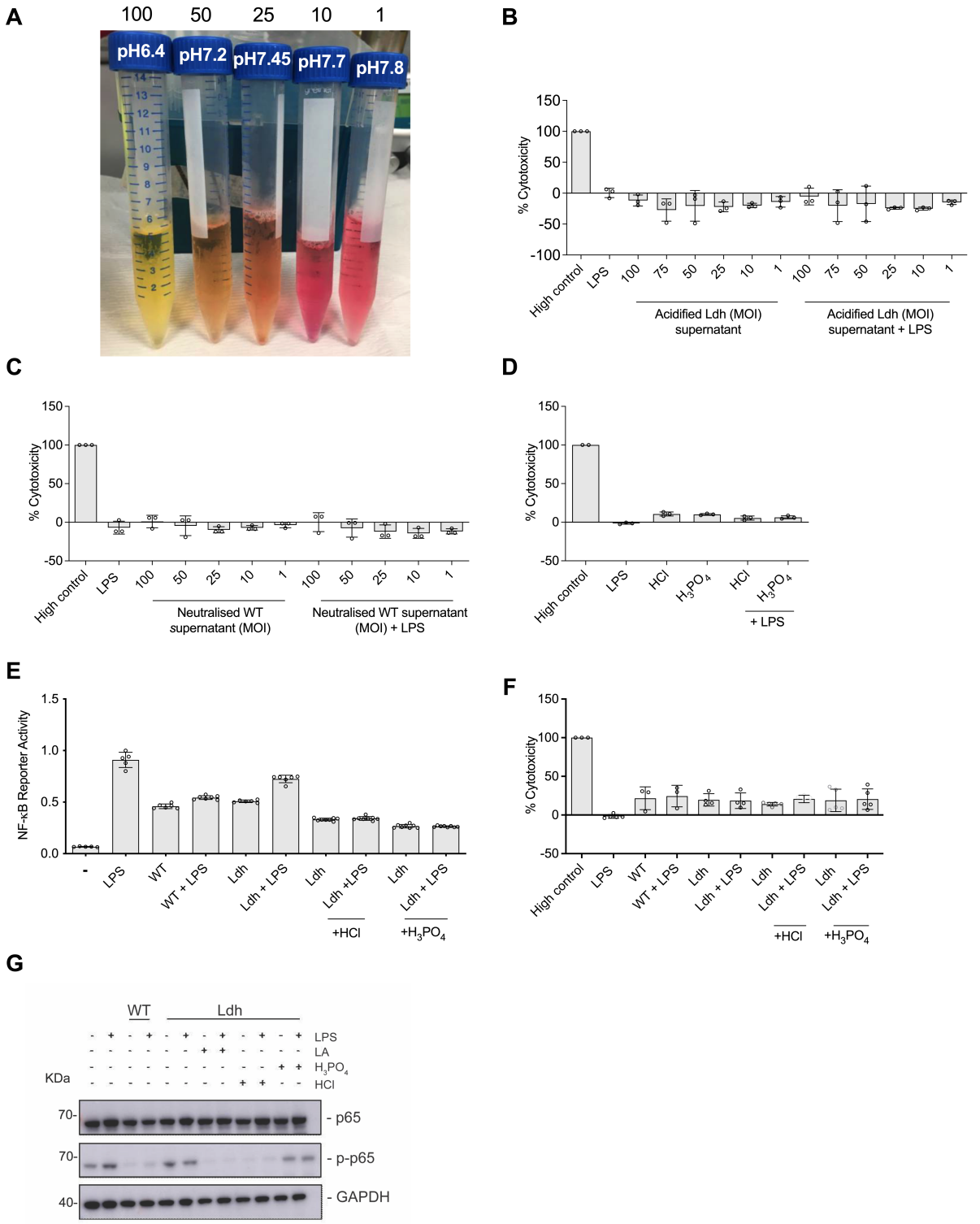

Figure S5 – pH adjusted medium does not affect macrophages viability.

(A) Picture of bacterial-free supernatant at indicated MOI. The colour indicator in the cell culture medium turns yellow upon acidification. RAW 264.7 macrophages were incubated with **(B)** acidified bacterial-free Ldh supernatant, **(C)** neutralised bacterial-

1278 free WT supernatant, **(D)** acidified cell media in the absence of bacteria, and **(E, F)**
1279 WT *E. faecalis* or Ldh deletion mutant treated concurrently with LPS at specific MOI
1280 for 6 h prior to measurement of NF-κB or LDH activity. **(B-D, F)** Triton-X treatment
1281 served as a positive control (high control) for cell death. **(E-F)** RAW 264.7
1282 macrophages incubated with WT or Ldh mutant were also supplemented with different
1283 acids to acidify the pH for the duration of the experiment prior to measurement of NF-
1284 κB-driven SEAP reporter activity. **(B-F)** Data (mean ± SEM) are a summary of at least
1285 three independent experiments. **(G)** Western blots were performed on protein
1286 extracted from RAW 264.7 macrophages infected with WT or Ldh that were incubated
1287 in acidified cell culture media in the presence or absence of LPS for 6 h and probed
1288 with antibodies specific for p65, p-p65, and GAPDH. Cell culture media was acidified
1289 to pH 6.4 with lactic acid and with the inorganic acids H_3PO_4 and HCl. Data shown are
1290 representative of at least 3 independent experiments.

1291
1292
1293
1294
1295
1296
1297
1298
1299
1300
1301
1302

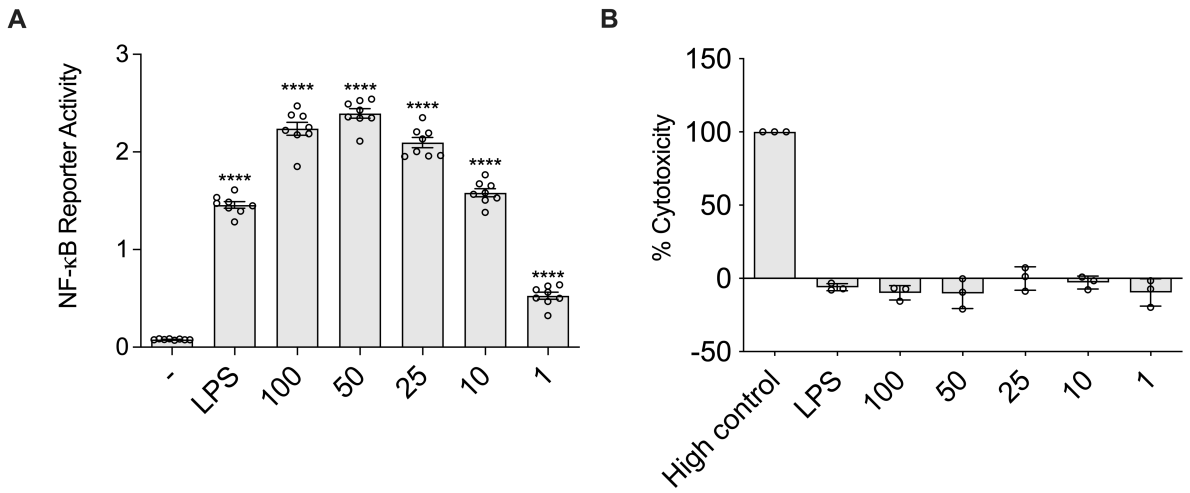

Figure S6 – Intracellular *E. faecalis* do not contribute to NF-κB suppression in macrophages.

RAW 264.7 macrophages was incubated with *E. faecalis* wildtype (MOI 100, 50, 25, 10, 1) 3 h and treated with 500 µg/mL of gentamicin with penicillin G overnight at 37˚C prior to measurement of **(A)** NF-κB-driven SEAP reporter activity and **(B)** LDH assay. Data (mean ± SEM) are a summary of at least three independent experiments. Statistical analysis was performed using one-way ANOVA with Tukey's multiple with comparison where ****$p<0.0001$ as compared to media control.

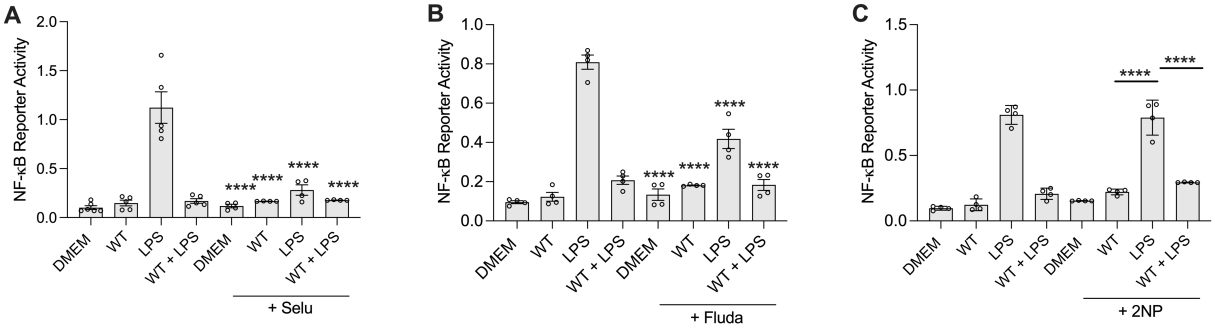

Figure S7 – STAT1 does not play a role in suppressing NF-κB in *E. faecalis* infection.

RAW 264.7 macrophages were infected with the WT *E. faecalis* and incubated with cell culture media in presence or absence of LPS and **(A)** Selu (1 μM) and **(B)** Fluda (10 μM) and **(C)** 2NP (45 μM) for 6 h prior to measurement of NF-κB-driven SEAP reporter activity. The compounds were added 30 min before the beginning of the experiment. Data (mean ± SEM) are a summary of at least three independent experiments. Statistical analysis was performed using one-way ANOVA with Tukey's multiple comparison tests where ****$p<0.001$ as compared to LPS unless otherwise indicated.

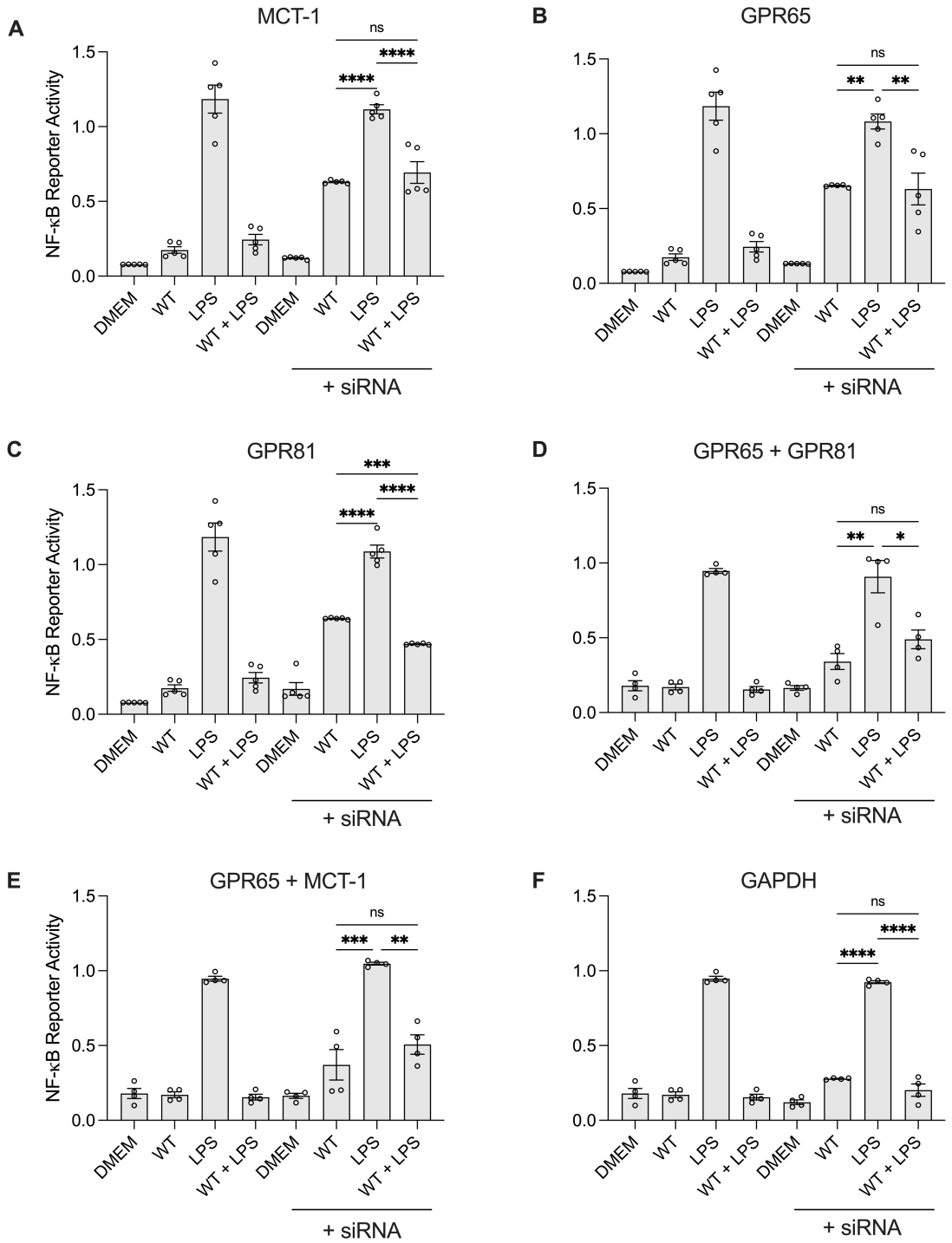

1336
1337 **Figure S8 – The lactate transporters MCT-1 and GPR81 are redundant in their**
1338 **role in the suppression of NF-κB activation of *E. faecalis* infection.** RAW 264.7
1339 macrophages, with successfully silenced lactate transporters as indicated, were
1340 infected with the wildtype *E. faecalis* and incubated with cell culture media in the
1341 presence or absence of LPS for 6 h prior to measurement of NF-κB-driven SEAP

reporter activity. Silencing the expression of *Mct-1*, *Gpr81* and *Gpr65* alone or in combination was achieved by siRNA. Data (mean ± SEM) are a summary of three independent experiments. *Gapdh* was also silenced as a control for adverse effects of the technique. Statistical analysis was performed using ordinary one-way ANOVA followed by Tukey's multiple comparison test ns, $p>0.05$; *$p\leq0.05$; and **$p<0.01$; ***$p<0.001$ and ****$p<0.001$.

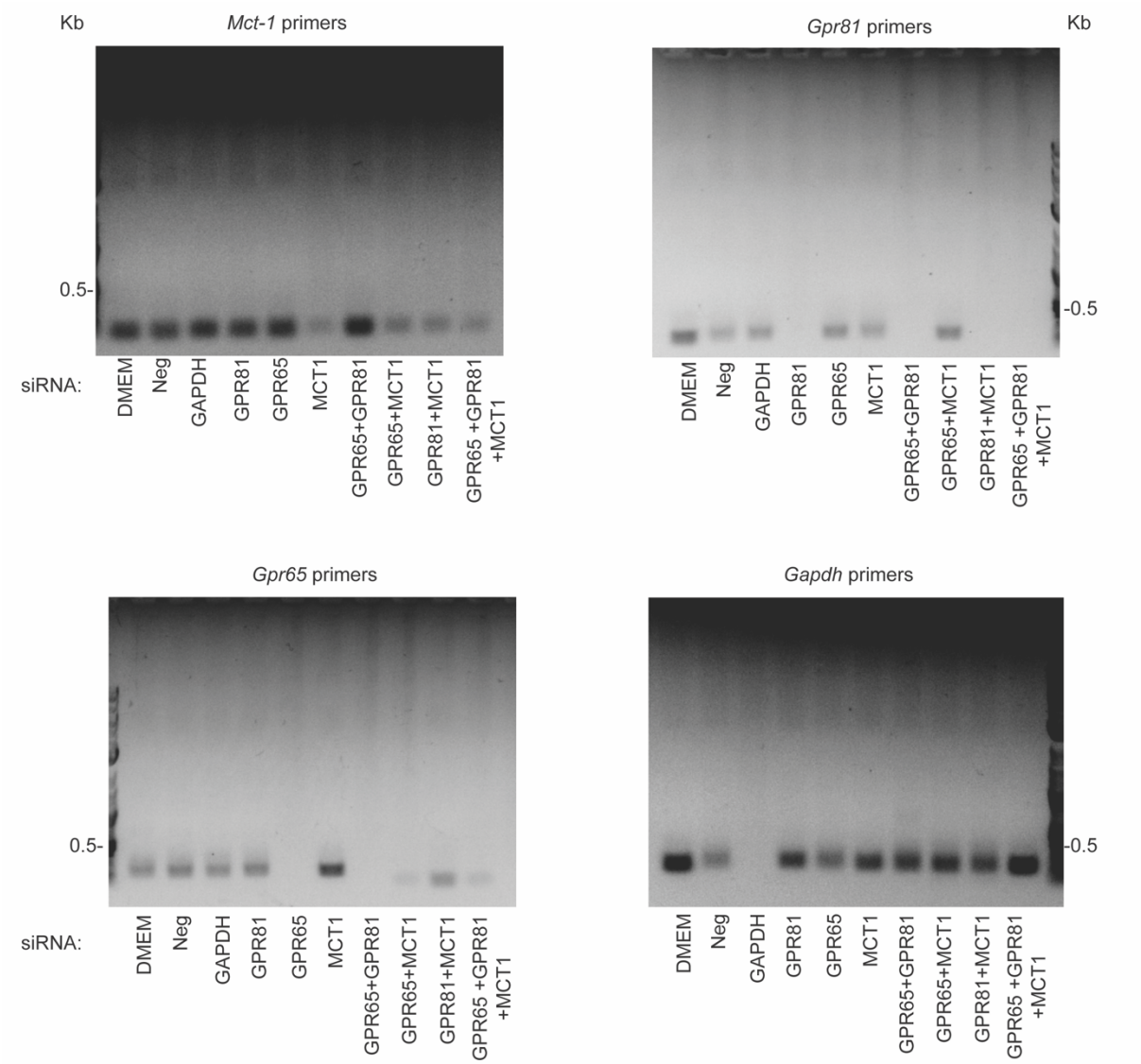

Figure S9 – Successful knockdown of lactate transporters of interest was verified with RT-PCR. Transcript levels of the silenced genes of interest were assessed with specific primers for each target. Negative control used was the Silencer

Select Negative Control siRNAs that contain siRNAs with sequences that do not target any gene product.

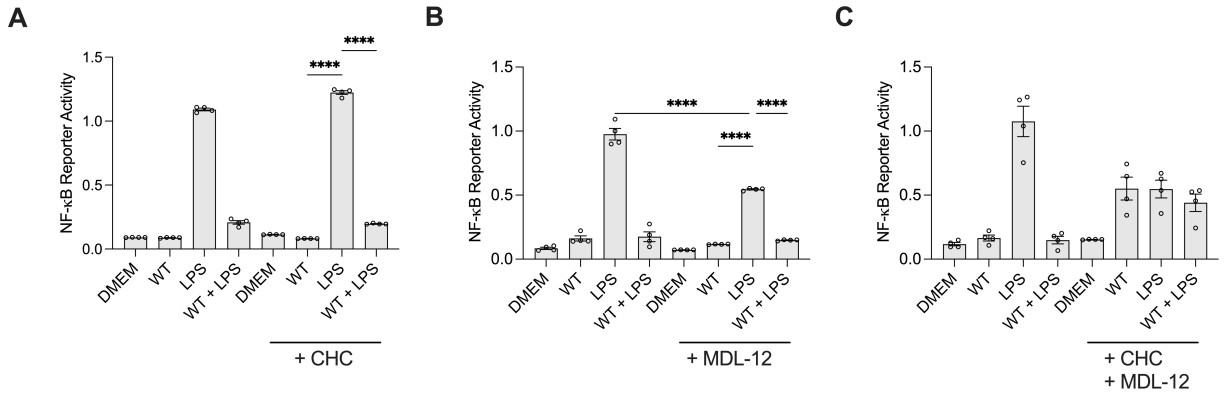

Figure S10 – MCT1 and GPCR sensors mediate *E. faecalis* suppression of NF-κB activation in macrophages. RAW 264.7 macrophages were infected with the WT *E. faecalis* and incubated in cell culture media in presence or absence of LPS and **(A)** CHC (5 mM) and **(B)** MDL-12 (20 μM) and **(C)** CHC + MDL-12 for 6 h prior to measurement of NF-κB-driven SEAP reporter activity. The compounds were added 30 min before the beginning of the experiment. Data (mean ± SEM) are a summary of at least three independent experiments. Statistical analysis was performed using one-way ANOVA with Tukey's multiple comparison tests where NS, $p>0.05$ and ****$p<0.001$.

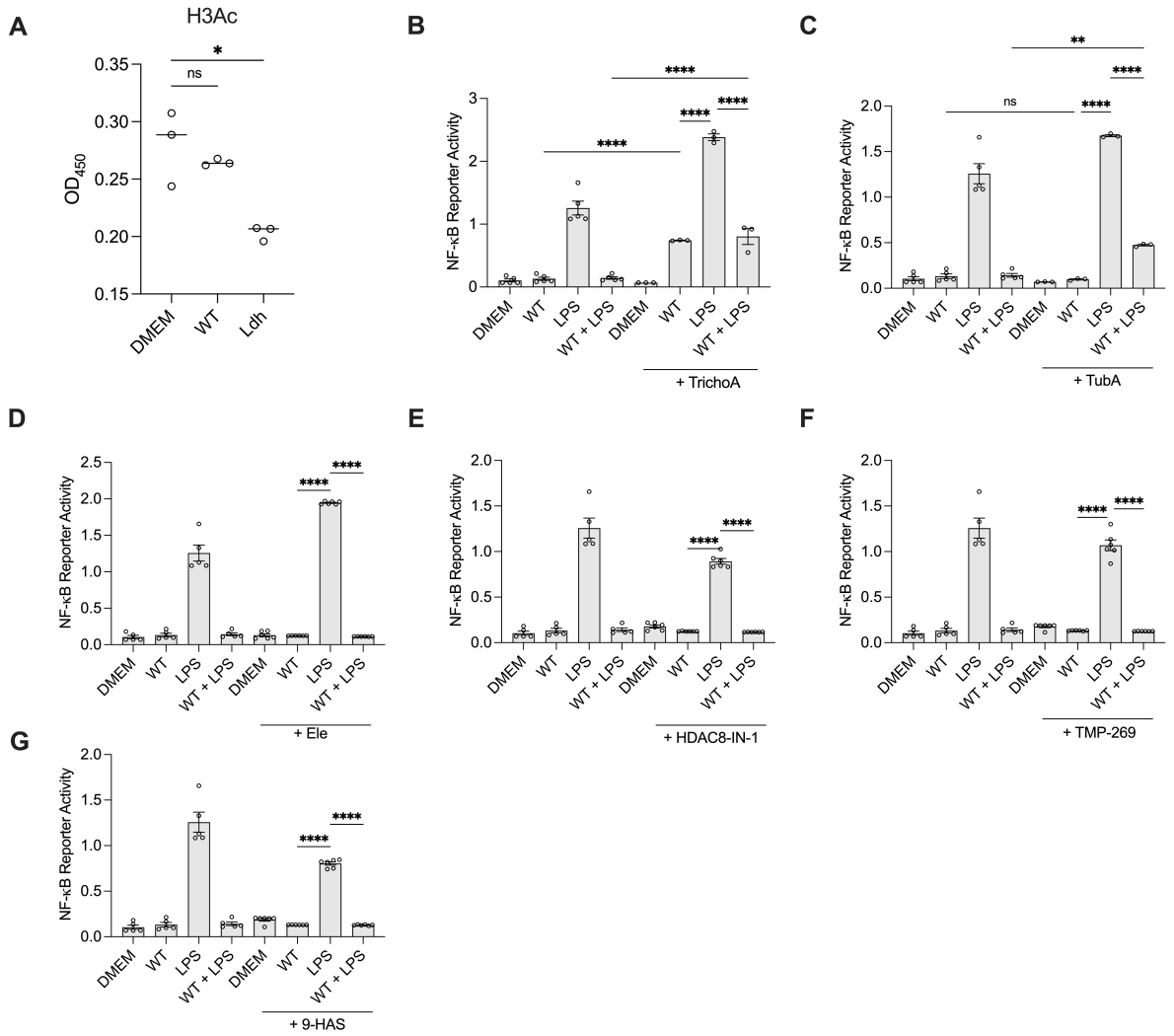

Figure S11 – HDACs likely play a partial role in mediating *E. faecalis* suppression of NF-kB activation in macrophages. (A) Relative abundance of H3Ac by ELISA of uninfected or WT and Ldh infected macrophages. RAW 264.7 macrophages were infected with the WT strain and incubated with cell culture media in the presence or absence of LPS and **(B)** TrichoA (10 nM) and **(C)** TubA (15 nM), **(D)** Ele (1 μM), **(E)** HDAC8-IN-1 (100 nM), **(F)** TMP-269 (10 μM) and **(G)** 9-HAS (100 μM) for 6 h prior to measurement of NF-κB-driven SEAP reporter activity. The compounds were added 30 min before the beginning of the experiment. Data (mean ± SEM) are a summary of at least three independent experiments. Statistical analysis was performed using one-way ANOVA with Tukey's multiple comparison tests where ns, $p>0.05$; *$p\leq0.05$; and ****$p<0.001$.

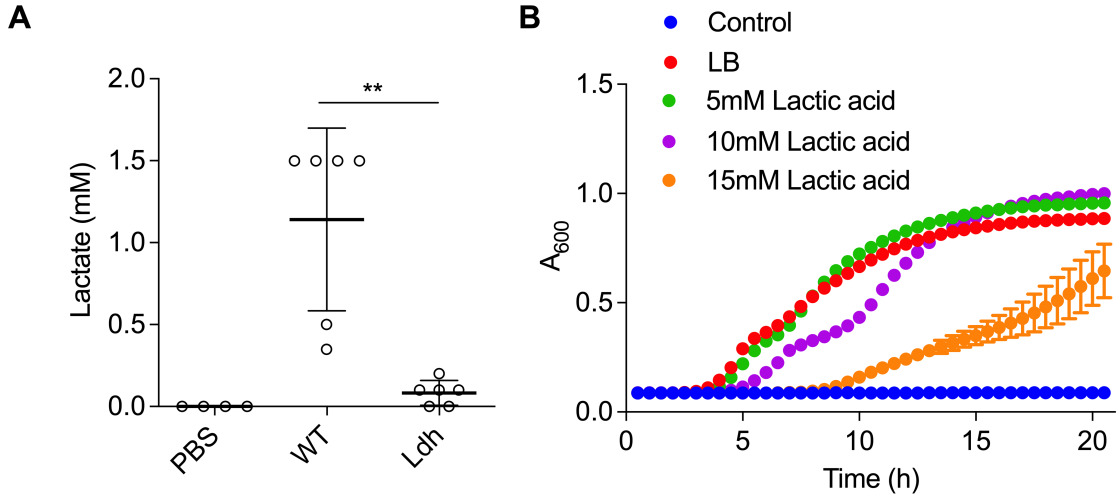

Figure S12 – Lactic acid does not promote *E. coli* growth at tested concentrations.

Lactate concentration of wound measured at **(A)** 24 hpi for the indicated condition. **(B)** Growth curve for *E. coli* strain UTI89 grown overnight in LB media supplemented with different concentration of lactate.

1416 **Supplementary Tables**

1417 **Table S1 –** Differentially expressed NF-κB/ AP-1-related genes

		Condition					
		Uninfected LPS-treated vs uninfected untreated		**MOI 100 untreated vs uninfected untreated**		**MOI 100 LPS-treated vs uninfected LPS-treated**	
Gene	**Gene product**	**Log2FC**	**Significant?**	**Log2FC**	**Significant?**	**Log2FC**	**Significant?**
NF-κB							
Tlr4	TLR4	-0.84	No	-0.66	No	-1.33	No
Cd14	CD14	2.15	Yes	0.31	No	-2.13	Yes
Myd88	MyD88	1.11	No	-1.06	No	-1.86	Yes
Tirap	TIRAP	0.38	No	-1.03	No	-1.16	No
Ly96	MD-2	0.89	No	0.29	No	-0.14	No
Ticam1	TRIF	1.84	No	1.59	Yes	0.28	No
Ticam2	TRAM	-1.35	No	1.28	No	2.48	Yes
Traf6	TRAF6	0.46	No	0.57	No	-0.09	No
Map3k7	TAK1	-0.06	No	0.07	No	0.17	No
Chuk	IKKα	0.32	No	0.35	No	0.004	No
Ikbkb	IKKβ	0.37	No	-0.02	No	-0.13	No
Nfkbia	IKBα	2.95	Yes	3.01	Yes	0.95	No
Rel	p65	1.60	Yes	3.55	Yes	0.29	No
Nfkb1	p105	3.20	Yes	2.33	Yes	0.11	No
Nfkb2	p100	1.98	Yes	1.84	Yes	0.89	No
AP-1							
Mapk14	p38	-0.62	No	-1.87	Yes	-0.94	No
Mapk8	JNK	0.28	No	0.54	No	0.40	No
Jun	cJun	0.47	No	0.82	No	-0.34	No
Fos	cFos	0.39	No	-0.65	No	-1.79	Yes
Common							
Rps6ka5	MSK1	-2.58	Yes	-1.87	Yes	-0.99	No
Rps6ka4	MSK2	0.29	No	-0.30	No	0.22	No
Mapk1	ERK	-0.09	No	0.11	No	0.05	No

1418
1419
1420
1421
1422
1423
1424
1425
1426
1427
1428
1429
1430
1431
1432
1433
1434

1435 **Table S2-** List of hits after transposon screen for genes that contribute to suppress
1436 NF-κB activation in macrophages

Gene	Gene product	Locus tag
OG1RF_10013	Adenylosuccinate synthase	OG1RF_10013
mptD	Mannose PTS enzyme IID component	OG1RF_10021
ldh1	L-lactate dehydrogenase 1	OG1RF_10199
OG1RF_10329	PaaI family thioesterase	OG1RF_10329
OG1RF_10418	YlbF family regulator	OG1RF_10418
pptB	ABC-family peptide pheromone efflux transporter, membrane protein	OG1RF_10427
rpoN	RNA polymerase factor sigma-54	OG1RF_10514
pgmB	β-phosphoglucomutase	OG1RF_10682
dapA	4-hydroxy-tetrahydrodipicolinate synthase	OG1RF_10956
yycH	YycH protein	OG1RF_10967
trpX	Tryptophan ABC transporter substrate-binding protein	OG1RF_11022
OG1RF_11023	ABC transporter permease	OG1RF_11023
OG1RF_11036	Putative transporter, P-type ATPase family	OG1RF_11036
OG1RF_11131	ABC transporter ATP-binding protein/permease	OG1RF_11131
nrnA	5'-3' exonuclease NrnA	OG1RF_11161
OG1RF_11270	Hypothetical protein	OG1RF_11270
aroE	Shikimate dehydrogenase	OG1RF_11280
aroC	Chorismate synthase	OG1RF_11283
tkt	Transketolase	OG1RF_11300
pflB	Formate C-acetyltransferase	OG1RF_11329
lepB	Signal peptidase I	OG1RF_11391
pbp1B	putative bifunctional peptidoglycan glycosyltransferase/DD-transpeptidase, penicillin-binding protein 1B	OG1RF_11450
OG1RF_11602	Putative transporter, P-type ATPase family	OG1RF_11602
dcm	DNA (cytosine-5-)-methyltransferase	OG1RF_11622
relA	Bifunctional (p)ppGpp synthase/hydrolase	OG1RF_11636
OG1RF_11669	DUF1033 family protein	OG1RF_11669
efaC	Mn^{2+} ABC transporter ATP-binding protein	OG1RF_11677
efrE	ABC family efflux transporter ATP-binding protein/permease EfrE	OG1RF_11766
OG1RF_11854	Metalloregulator ArsR/SmtB family transcription factor	OG1RF_11854
OG1RF_11923	Hypothetical protein	OG1RF_11923
OG1RF_12024	ABC transporter ATP-binding protein	OG1RF_12024
OG1RF_12033	ATP-dependent RecD-like DNA helicase	OG1RF_12033
OG1RF_12043	ClpXP adapter SpxH family protein	OG1RF_12043
OG1RF_12058	SMC family ATPase	OG1RF_12058
OG1RF_12066	5-bromo-4-chloroindolyl phosphate hydrolysis family protein	OG1RF_12066
OG1RF_12113	ABC transporter permease	OG1RF_12113
OG1RF_12190	YkuJ family protein	OG1RF_12190
OG1RF_12284	Putative transporter, sulfate permease family	OG1RF_12284
ireP	PP2C-type protein-serine/threonine phosphatase	OG1RF_12385
def	Peptide deformylase	OG1RF_12388
OG1RF_12401	Gluconate-specific PTS enzyme IID component	OG1RF_12401
OG1RF_12446	ArgE/DapE family deacylase	OG1RF_12446
OG1RF_12459	Isochorismatase/nicotinamidase	OG1RF_12459

menA	1,4-dihydroxy-2-naphthoate polyprenyltransferase	OG1RF_12507
croS	HAMP domain-containing sensor histidine kinase	OG1RF_12536
citE	Citrate (pro-3S)-lyase subunit beta	OG1RF_12565
citC	[citrate (pro-3S)-lyase] ligase	OG1RF_12567

Table S3 – Cytotoxicity as measured by LDH assay of compounds used in this study.

Condition	% Cytotoxicity	Source
DMEM (Baseline)	5.15	Gibco
Stattic (10 μM)	14.92	MedChemExpress
ML115 (1 μM)	12.01	MedChemExpress
2NP (45 μM)	25.34	MedChemExpress
Selu (1 μM)	15.33	MedChemExpress
Fluda (40 μM)	12.01	MedChemExpress
CHC (5 mM)	15.54	MedChemExpress
MDL-12 (20 μM)	11.58	MedChemExpress
TrichoA (10 nM)	19.47	MedChemExpress
TubA (15 nM)	4.92	MedChemExpress
Ele (1 μM)	5.54	MedChemExpress
HDAC8-IN-1 (100 nM)	5.01	MedChemExpress
TMP-269 (10 μM)	26.12	MedChemExpress
9-HAS (100 μM)	27.80	MedChemExpress

1466 **Table S4-** List of primers used in this study

Gene	Oligo Name	Sequence 5' to 3'
ldh deletion		
ldh1	dLDH1_For	CATGCTCGAGCGGCCATTATATGTTGGCACATCCAGG
	dLDH1_Rev	CAGTGTGCTGGAATTAATTTAACGCACTCACTCGAT
	dLDH1_SewF	AAGCGGAGTAACAATAGTGGGTAGCTCTTACATGTGCGTAAT
	dLDH1_SewR	ATTACGCACATGTAAGAGCTACCCACTATTGTTACTCCGCTT
	LDH1_F	GAAGAATAAATTAACCATTGCTTCTTCATC
	LDH1_R	CTTATCTCACGCATTAGCATTTAC
ldh2	dLDH2_For	CATGCTCGAGCGGCCGTCGTTTACTCTGTCCATCATTT
	dLDH2_Rev	CAGTGTGCTGGAATTTTTTCATTGTCCAGACCGAT
	dLDH2_SewF	ATAATCGCGTTGTGTACTTCACACGAACTTTTTAGGTGTGGTT
	dLDH2_SewR	AACCACACCTAAAAAGTTCGTGTGAAGTACACAACGCGATTAT
	LDH2_F	GAGGCAATTACTAAAATTCCATCAAAAC
	LDH2_R	CAATTGACTTATTAGATGGTGTGTCTT
ChIP-qPCR		
Myd88 (R1)	M_STAT3_1_F	GGCCCCGTAGTCTAG
	M_STAT3_1_R	CGCCTGTGGAGTTTC
Myd88 (R2)	M_STAT3_2_F	GGAAGCCAATCGTAATG
	M_STAT3_2_R	AAGGGGAGGGACTCC
Myd88 (R3)	M_STAT3_3_F	GCATCGGTGAGGAAAC
	M_STAT3_3_R	CCTCCCTAGCGCACC
Gapdh	M_gapdh_F	GCCCTTCTACAATGCCAAAG
	M_gapdh_R	TTGTGATGGGTGTGAACCAC
siRNA RT-PCR		
Hcar1	GPR81_M_F	GGTGGCACGATGTCATGTT
	GPR81_M_R	GACCGAGCAGAACAAGATGATT
SLC16A1	MCT1_M_F	TTGTCTGTCTGGTTGCGGCTTGATCG
	MCT1_M_R	CACCTCCAATAACACCAATG
Gpr65	GPR65_M_F	TGCGGCACAACCAAGCCACGGA
	GPR65_M_R	ATGTCGCGCTCTAAAACGCAGCG

1467